Improving CRISPR-Cas9 mediated genome integration in interspecific hybrid yeasts

Bennis, Nicole X.; Kostanjšek, Matic; van den Broek, Marcel; Daran, Jean Marc G.

DOI
10.1016/j.nbt.2023.04.001

Publication date
2023

Document Version
Final published version

Published in
New Biotechnology

New BIOTECHNOLOGY 76 (2023) 49–62

Contents lists available at ScienceDirect

New BIOTECHNOLOGY

journal homepage: www.elsevier.com/locate/nbt

Improving CRISPR-Cas9 mediated genome integration in interspecific hybrid yeasts

Nicole X. Bennis [1], Matic Kostanjšek [2], Marcel van den Broek [3], Jean-Marc G. Daran [*,4]

Department of Biotechnology, Delft University of Technology, van der Maasweg 9, 2627 HZ Delft, The Netherlands

ARTICLE INFO

Keywords:
Saccharomyces pastorianus
CRISPR-Cas9
Loss of heterozygosity
Landing sites
Genome modifications
Allo-aneuploid

ABSTRACT

Saccharomyces pastorianus is not a classical taxon, it is an interspecific hybrid resulting from the cross of *Saccharomyces cerevisiae* and *Saccharomyces eubayanus*. Exhibiting heterosis for phenotypic traits such as wort α-oligosaccharide consumption and fermentation at low temperature, it has been domesticated to become the main workhorse of the brewing industry. Although CRISPR-Cas9 has been shown to be functional in *S. pastorianus*, repair of CRISPR-induced double strand breaks is unpredictable and preferentially uses the homoeologous chromosome as template, preventing targeted introduction of the desired repair construct. Here, we demonstrate that lager hybrids can be edited with near 100% efficiency at carefully selected landing sites on the chimeric *SeSc*CHRIII. The landing sites were systematically selected and evaluated for (i) absence of loss of heterozygosity upon CRISPR-editing, (ii) efficiency of the gRNA, and (iii) absence of effect on strain physiology. Successful examples of highly efficient single and double gene integration illustrated that genome editing can be applied in interspecies hybrids, paving the way to a new impulse to lager yeast strain development.

Introduction

With an annual production of almost 2 billion hectolitres, lager beer is the world's most consumed alcoholic beverage (https://www.statista.com/). The workhorse for lager beer production is the yeast *Saccharomyces pastorianus*, a hybrid yeast that has emerged from a natural hybridization event, probably occurring during the Middle Ages, between the mesophilic ale yeast *Saccharomyces cerevisiae* and the cryotolerant yeast *Saccharomyces eubayanus* [1–3]. Hitherto most research aiming at improving the brewing performance of lager strains has been based on classical strain improvement [4–11]. Brewing strains resulting from these techniques are regarded as non-genetically modified organisms. Although these techniques proved their efficiency, they are time consuming and unpredictable, thus limiting the pace of strain development. Conversely molecular techniques and targeted genetic modifications would offer a faster alternative to creating specific mutants that might exhibit better brewing characteristics. The deployment of genetic engineering improvement strategies in the brewing industry is, however, impeded by three factors. The first is the producers' concerns about consumer acceptance of beers brewed with genetically modified yeasts [12]. While it is difficult to predict whether these reservations will last, in North America, yeasts-producing companies are already marketing modified ale and even lager strains (https://berkeleyyeast.com/, https://www.lallemandbrewing.com/) demonstrating that opinions are changing. The second point concerns the limited genetic accessibility of these hybrid yeasts, a trait likely related to the complex structure of their genome. Thirdly, the breweries have to deal with the regulatory implications for production with genetically

Abbreviations: CRISPR, Clustered Regularly Interspaced Short Palindromic Repeats; CHR, CHRomosome; gRNA, guide-RNA; DSB, Double Strand Break; LOH, Loss Of Heterozygosity; YPD, Yeast extract Peptone Dextrose; LB, Lysogeny Broth; HH, HammerHead; HDV, Hepatitis Delta Virus; FSC, Forward SCatter; SSC, Side Scatter; FACS, Fluorescence-Activated Cell Sorting; HPLC, High-Performance Liquid Chromatography; GC, Gas Chromatography; FID, Flame Ionization Detector; WGS, Whole Genome Sequencing.

* Corresponding author.
E-mail addresses: N.X.Bennis@tudelft.nl (N.X. Bennis), matic.kostanjsek@wur.nl (M. Kostanjšek), marcel.vandenbroek@tudelft.nl (M. van den Broek), J.G.Daran@tudelft.nl (J.-M.G. Daran).
[1] 0000-0002-3403-0844
[2] 0000-0002-6048-8533
[3] 0000-0002-7734-582X
[4] 0000-0003-3136-8193

https://doi.org/10.1016/j.nbt.2023.04.001
Received 23 December 2022; Received in revised form 3 March 2023; Accepted 4 April 2023
Available online 5 April 2023

modified organisms (GMOs), depending on their location in the world.

The hybrid nature of the *S. pastorianus* genome was confirmed for the first time with the genome sequence of the *S. pastorianus* Weihenstephan 34/70 strain [1]. This initial work was followed by multiple other *S. pastorianus* strain sequencing projects [13–16] that confirmed that lager yeast harbored an allo-aneuploidy genome. Although strain to strain variations exist, the lager yeast genome comprises both parental chromosome sets which all have different copy numbers. In addition to the presence of multiple copies, each chromosome has a homoeologous chromosome, which derives from the other parental species [17]. For example, the *S. cerevisiae* CHRI is a homoeolog of the *S. eubayanus* CHRI, which shares both high sequence similarity and gene syntheny [16,18]. This co–occurrence has likely contributed to translocation and loss of heterozygosity (LOH) events between chromosomes of the two sub-genomes (*ScSe* and *SeSc*) in *S. pastorianus* that are considered as hall-marks of domestication [15,19].

While this dual genome composition has promoted the emergence of essential phenotypic traits of lager brewing yeasts, the presence of homoeologous chromosome pairs has impaired genetic amenability [20]. This effect is even stronger when genome editing tools such as CRISPR-Cas9 are used. CRISPR-Cas endonucleases can simply target specific DNA sequences based on the user-defined composition of the single guide RNA (gRNA) sequence and presence of the protospacer adjacent motif (PAM) [21–24]. The CRISPR-Cas induced double strand breaks (DSB) are extremely recombinogenic and are resolved by the yeast homology directed repair (HDR) machinery, that uses native or foreign DNA containing sequence homology as repair template, thereby producing the desired genetic edit [25].

Although the CRISPR-Cas9 methodology has been successfully applied in *S. pastorianus* [26], it appeared in many situations that the editing outcome is unpredictable and characterization of the resulting edited locus has proven troublesome [20]. Whereas, in homozygous diploid yeasts, the gRNA programmed Cas9 introduces DSBs on both copies, in hybrid yeasts, gRNA are not necessarily designed to cut at all parental alleles. In this latter situation, the uncut homoeologous locus competes with the provided repair DNA fragments, facilitating chromosome recombination and reduced editing efficiency, resulting in loss of heterozygosity and even more undesired genetic changes [20].

The aim of this study is to improve the genetic accessibility of the allo-aneuploid yeast *S. pastorianus* by identifying unique landing sites devoid of homoeologous regions using a systematic approach. We evaluate whether the approach eliminates LOH when performing precise genome editing with CRISPR-Cas9. Identifying and targeting unique sequences offers opportunities for increased genetic engineering efficiencies in allo-aneuploid yeast. To demonstrate this, integration efficiency of single and double genes is tested.

Materials and methods

Strains and cultivation conditions

All yeast strains used in this study are listed in Table 1. Yeasts were grown on complex medium that contained 10 g·L^{-1} bacto yeast extract, 20 g·L^{-1} bacto peptone and 20 g·L^{-1} glucose (YPD). For selection of transformants or when selective pressure was required, YPD medium was supplemented with 200 mg·L^{-1} of hygromycin (YPD hyg). Solid YPD media was obtained by addition of 20 g·L^{-1} bacto agar. *S. cerevisiae* and *S. pastorianus* strains were cultivated at 30 °C and 20 °C, respectively while shaking at 200 rpm in an Innova 43/43 R incubation shaker (Brunswick, Nijmegen, the Netherlands). On solid media, *S. cerevisiae* and *S. pastorianus* strains were cultivated on agar plates at 30 °C and 20 °C, respectively. Fermentations were performed with full malt wort at either 17° P or 5.7° P (Heineken, Zoeterwoude, The Netherlands) supplemented with 1 mL·L^{-1} pluronic acid.

Escherichia coli XL1-Blue (New England Biolabs, Ipswich, MA, USA) cultures were grown in 15 mL Greiner tubes containing 5 mL lysogenic broth (LB) medium supplemented with 10 mg·L^{-1} ampicillin (LB Amp), 50 mg·L^{-1} kanamycin (LB Kan) or 10 mg·L^{-1} chloramphenicol (LB Cam) for selection and cultivated at 37 °C. Solid medium was prepared by addition of 20 g·L^{-1} bacto agar to the medium. Frozen stock cultures of *S. cerevisiae*, *S. pastorianus* and *E. coli* strains were prepared by addition of 30% (v/v) glycerol and stocks were stored as 1 mL aliquots at − 80 °C.

Molecular biology techniques

PCR amplifications for cloning purposes and diagnostic PCRs were performed as described in [20]. All plasmids and primers (Sigma Aldrich, Zwijndrecht, The Netherlands) constructed or used in this study are listed in Tables 2 and 3, respectively. Golden Gate cloning was performed using 25 fmol of each fragment with BsmBI or *Bsa*I restriction enzymes (New England Biolabs) according to [27,28]. Gibson Assembly was performed with 200 fmol of each fragment using NEBuilder® HiFi DNA Assembly Master Mix (New England BioLabs) and one hour incubation at 50 °C [29]. Constructed plasmids were transformed into *E. coli* XL1-blue (New England Biolabs) chemically competent cells.

CRISPR-Cas9 plasmid construction

The gRNA sequences for the introduction in iCas9 platform plasmid pUDP002 [30] were designed in such a way that they yield compatible sticky ends for ligation upon restriction with *Bsa*I, following the Golden Gate cloning strategy for gRNA cloning described in [26]. The plasmids pUD1205-pUD1209, pUD1243, pUD1244, pUD1212 and pUD1213

Table 1
Strains used in this study.

Species	Strain	Relevant genotype	Origin
S. cerevisiae	CEN.PK113–7D	MATa *MAL2–8c SUC2*	[69]
S. pastorianus	CBS 1483	Group II brewer's yeast, Heineken bottomyeast, isolated July 1927	[70]
S. pastorianus	WS 34/70-AE1	Group II brewer's yeast, flocculent yeast	[1]
S. pastorianus	IMK1062	CBS 1483 Δ*ScEEB1*::ymNeongreen (LOH), colony 1	This study
S. pastorianus	IMK1063	CBS 1483 Δ*ScEEB1*::ymNeongreen (LOH), colony 3	This study
S. pastorianus	IMK1064	CBS 1483 Δ*ScEEB1*::ymNeongreen (LOH), colony 4	This study
S. pastorianus	IMK1065	CBS 1483 Δ*ScEEB1*::ymNeongreen (LOH), colony 6	This study
S. pastorianus	IMI504	CBS 1483 Δ*Se*YCL049C::ymNeongreen	This study
S. pastorianus	IMI505	CBS 1483 Δ*Se*YCL036W::ymNeongreen	This study
S. pastorianus	IMI506	CBS 1483 Δ*Se*YCL012C::ymNeongreen	This study
S. pastorianus	IMI507	CBS 1483 Δ*Sc*YCR051W::ymNeongreen	This study
S. pastorianus	IMI508	CBS 1483 Δ*Sc*YCR087C-A::ymNeongreen	This study
S. pastorianus	IMI509	CBS 1483 Δ*Se*Site1::ymNeongreen	This study
S. pastorianus	IMI510	CBS 1483 Δ*Se*Site2::ymNeongreen	This study
S. pastorianus	IMI511	CBS 1483 Δ*Se*Site3::ymNeongreen	This study
S. pastorianus	IMI512	CBS 1483 Δ*Se*Site4::ymNeongreen	This study
S. pastorianus	IMI483	CBS 1483 Δ*Sc*YCR087C-A::*TDH3*p-*BbaldC-ENO1*t	This study
S. pastorianus	IMI485	CBS 1483 Δ*Sc*YCR087C-A::*TDH3*p-*LlaldC-ENO1*t	This study

Table 2
Plasmids used in this study.

Plasmid	Genotype[a]	Reference
pUDP002	ori ampR panARS$^{(OPT)}$ *AgTEF1*p-*hph*-*AgTEF1*t *ScTDH3*p-$^{BsaI\text{-}BsaI}$-*ScCYC1*t *AaTEF1*p-*Spycas9*$^{D147Y\ P411T}$-*ScPHO5*t	[30]
pUD1205	ori kanR^{BsaI}HH-gRNA$_{SeYCL049C}$-HDV^{BsaI}	GeneArt
pUD1206	ori kanR^{BsaI}HH-gRNA$_{SeYCL036W}$-HDV^{BsaI}	GeneArt
pUD1207	ori kanR^{BsaI}HH-gRNA$_{SeYCL012C}$-HDV^{BsaI}	GeneArt
pUD1208	ori kanR^{BsaI}HH-gRNA$_{ScYCR051W}$-HDV^{BsaI}	GeneArt
pUD1209	ori kanR^{BsaI}HH-gRNA$_{ScYCR087C\text{-}A}$-HDV^{BsaI}	GeneArt
pUD1243	ori kanR^{BsaI}HH-gRNA$_{SeSite1}$-HDV^{BsaI}	GeneArt
pUD1244	ori kanR^{BsaI}HH-gRNA $_{SeSite2}$-HDV^{BsaI}	GeneArt
pUD1212	ori kanR^{BsaI}HH-gRNA $_{SeSite3}$-HDV^{BsaI}	GeneArt
pUD1213	ori kanR^{BsaI}HH-gRNA $_{SeSite4}$-HDV^{BsaI}	GeneArt
pUDP168	ori ampR panARS$^{(OPT)}$ *AgTEF1*p-*hph*-*AgTEF1*t *ScTDH3*p-HH-gRNA$_{ScEEB1}$-HDV-*ScCYC1*t *AaTEF1*p-*Spycas9*$^{D147Y\ P411T}$-*ScPHO5*t	This study
pUDP172	ori ampR panARS$^{(OPT)}$ *AgTEF1*p-*hph*-*AgTEF1*t *ScTDH3*p-HH-gRNA$_{ScEAT1}$-HDV-*ScCYC1*t *AaTEF1*p-*Spycas9*$^{D147Y\ P411T}$-*ScPHO5*t	This study
pUDP269	ori ampR panARS$^{(OPT)}$ *AgTEF1*p-*hph*-*AgTEF1*t *ScTDH3*p-HH-gRNA$_{SeYCL049C}$-HDV-*ScCYC1*t *AaTEF1*p-*Spycas9*$^{D147Y\ P411T}$-*ScPHO5*t	This study
pUDP270	ori ampR panARS$^{(OPT)}$ *AgTEF1*p-*hph*-*AgTEF1*t *ScTDH3*p-HH-gRNA$_{SeYCL036W}$-HDV-*ScCYC1*t *AaTEF1*p-*Spycas9*$^{D147Y\ P411T}$-*ScPHO5*t	This study
pUDP271	ori ampR panARS$^{(OPT)}$ *AgTEF1*p-*hph*-*AgTEF1*t *ScTDH3p*-HH-gRNA$_{SeYCL012C}$-HDV-*ScCYC1*t *AaTEF1*p-*Spycas9*$^{D147Y\ P411T}$-*ScPHO5*t	This study
pUDP272	ori ampR panARS$^{(OPT)}$ *AgTEF1*p-*hph*-*AgTEF1*t *ScTDH3*p-HH-gRNA$_{ScYCR051W}$-HDV-*ScCYC1*t *AaTEF1*p-*Spycas9*$^{D147Y\ P411T}$-*ScPHO5*t	This study
pUDP273	ori ampR panARS$^{(OPT)}$ *AgTEF1*p-*hph*-*AgTEF1*t *ScTDH3*p-HH-gRNA$_{ScYCR087C\text{-}A}$-HDV-*ScCYC1*t *AaTEF1*p-*Spycas9*$^{D147Y\ P411T}$-*ScPHO5*t	This study
pUDP283	ori ampR panARS$^{(OPT)}$ *AgTEF1*p-*hph*-*AgTEF1*t *ScTDH3*p-HH-gRNA$_{SeSite1}$-HDV-*ScCYC1*t *AaTEF1*p-*Spycas9*$^{D147Y\ P411T}$-*ScPHO5*t	This study
pUDP284	ori ampR panARS$^{(OPT)}$ *AgTEF1*p-*hph*-*AgTEF1*t *ScTDH3*p-HH-gRNA$_{SeSite2}$-HDV-*ScCYC1*t *AaTEF1*p-*Spycas9*$^{D147Y\ P411T}$-*ScPHO5*t	This study
pUDP276	ori ampR panARS$^{(OPT)}$ *AgTEF1*p-*hph*-*AgTEF1*t *ScTDH3*p-HH-gRNA$_{SeSite3}$-HDV-*ScCYC1*t *AaTEF1*p-*Spycas9*$^{D147Y\ P411T}$-*ScPHO5t*	This study
pUDP277	ori ampR panARS$^{(OPT)}$ *AgTEF1*p-*hph*-*AgTEF1*t *ScTDH3*p-HH-gRNA$_{SeSite4}$-HDV-*ScCYC1*t *AaTEF1*p-*Spycas9*$^{D147Y\ P411T}$-*ScPHO5*t	This study
pYTK009	*ori camR TDH3*p	[27]
pYTK051	*ori camR ENO1*t	[27]
pYTK053	ori camR *ADH1*t	[27]
pGGKp304	ori camR ymNeongreen	[31]
pGGKd015	ori ampR ConLS-GFPdo-ConR1	[71]
pGGKd034	ori ampR *2 μm hygR* ConLS-GFPdo-ConR1	This study
pUDE1111	ori ampR *2 μm hygR* ConLS-*TDH3*p-ymNeongreen-*ADH1*t-ConR1	This study
pUDE1112	ori ampR *2 μm hygR* ConLS-*TDH3*p-ymScarletI-*ADH1*t-ConR1	
pUD1218	ori ampR *TDH3*p-*BbaldC*-*ENO1*t	This study
pUD1220	ori ampR *TDH3*p-*LlaldC*-*ENO1*t	This study

(GeneArt, Thermo Fisher Scientific, Waltham, MA) contain the gRNA sequences targeting *Se*YCL049C, *Se*YCL036W, *Se*YCL012C, *Sc*YCR051W, *Sc*YCR087C-A, *Se*Site1, *Se*Site2, *Se*Site3 and *Se*Site4, respectively, and are flanked by the HammerHead (HH) and Hepatitis Delta Virus (HDV) ribozymes. Correct Golden Gate cloning of these gRNAs into the platform plasmid pUDP002 resulted in pUDP269-pUDP273, pUDP283, pUDP284, pUDP276 and pUDP277, which were verified by diagnostic PCR with primer 4068 binding to SHR I and primers 18516, 18521, 18526, 18531, 18536, 18541, 18546, 18551, 18556, 19067 and 19068 binding to the respective gRNA spacers. Cloning of the gRNAs targeting *ScEEB1* and *ScEAT1* into pUDP002, resulting in pUDP168 and pUDP172 was confirmed in a diagnostic PCR with primers 1153 and 580.

The plasmids pUDE1111 and pUDE1112 that express the ymNeongreen gene and the ymScarletI gene respectively, were constructed using Golden Gate cloning with plasmids pYTK009, pYTK053 [27], pGGKp034 (ymNeongreen [31]) or pGGKp032 (ymScarletI [31]) respectively, and pGGKd034 (Table 2). Correct construction of pUDE1111 and pUDE1112 was verified by diagnostic PCR with primers 10320 & 10325.

Construction of acetolactate decarboxylase gene expressing plasmids

aldC genes from *Brevibacillus brevis* (CP087980.1), excluding the secretion signal peptide, and *Leuconostoc lactis* (CP042420.1) were codon optimized for yeast, and ordered as synthetic genes (GeneArt, Thermo Fisher Scientific), resulting in plasmids pUD374 and pUD376. Genes were amplified from these plasmids using primer pairs 18759 & 18760 and 18763 & 18764, respectively, incorporating golden gate compatible flanks. Golden gate assembly with pGGKd015, pYTK009, pYTK051 and the PCR-amplified *aldC* gene fragment resulted in plasmids pUD1218 and pUD1220, respectively, for *BbaldC* and *EaaldC*, which were verified by diagnostic PCR using the primer pair 10320 & 10325.

CRISPR-Cas9 genome editing in S. pastorianus and S. cerevisiae strains

CRISPR-Cas9 genome editing in *S. pastorianus* strains was performed by transforming CBS 1483 or WS 34/70 with 500 ng gRNA plasmid and 1000 ng repair fragment (Table 4). As negative control, transformation from which the repair fragment was omitted was performed. Yeast transformation was performed by electroporation as described in [20]. The transformed cells were incubated in 0.5 mL YPD during 2 h, followed by re-suspending in 100 μL sterile demi-water and plating on selective medium. CRISPR-Cas9 genome editing in *S. cerevisiae* strain CEN.PK113–7D was performed by transforming 500 ng gRNA plasmid and 1000 ng repair fragment according to the LiAc/ss-DNA/PEG chemical transformation method [32].

The ymNeongreen integrations were performed by co-transforming the gRNA plasmid and the corresponding repair fragment consisting of the ymNeongreen expression cassette flanked by 60 bp homologous sequences for recombination. The ymNeongreen repair fragments were obtained by PCR amplification using pUDE1111 as template and primer pairs 18512 & 18513 for *Se*YCL049C, 18517 & 18518 for *Se*YCL036W, 18522 & 18523 for *Se*YCL012C, 18527 & 18528 for *Sc*YCR051W, 18532 & 18533 for *Sc*YCR087C-A, 18537 & 18538 for *Se*Site1, 18542 & 18543 for *Se*Site2, 18547 & 18548 for *Se*Site3 and 18552 & 18553 for *Se*Site4. The *aldC* gene expression cassettes for integration in YCR087C-A were obtained by PCR amplification with primers 18532 & 18533 using pUD1218 or pUD1220, respectively, as template.

In vivo assembled integration of ymNeongreen and ymScarletI was performed with two fragments to repair the CRISPR-induced DSB. The ymNeongreen fragment was amplified from pUDE1111 with primers 18512 & 18768 incorporating the *Se*YCL049C flank and the SHR CB flank, while the ymScarletI fragment was amplified from pUDE1112 with primers 13047 & 18513 incorporating the SHR CB and *Se*YCL049C flanks.

Yeast genomic DNA for diagnostic purposes was isolated using the lithium acetate (LiOAc)-SDS method [33]. Gene integrations in *Se*YLC049C were confirmed with primers 18514 & 18515, *Se*YCL036W with 18519 & 18520, *Se*YCL012C with 18990 & 18991, *Sc*YCR051W with 18529 & 18530, *Sc*YCR087C-A with 18534 & 18535, *Se*Site1 with 18539 & 18540, *Se*Site2 with 18544 & 18545, *Se*Site3 with 18549 & 18550, *Se*Site4 with 18992 & 18993, *ScEEB1* with 15944 & 15945 and *ScEAT1* with 15950 & 15951.

Flow cytometry and cell sorting

After the transformation procedure, the cell suspension was plated onto selective medium (1/5th of the cells) or transferred to 20 mL liquid selective medium in vented tubes (4/5th of the cells) and cultivated for 5

Table 3
Primers used in this study.

Number	Primer name	Sequence (5' -> 3')	Purpose
gRNA plasmid construction			
4068	Nic1_amp_Fwd	GCCTACGGTTCCCGAAGTATGC	Diagnostic primer gRNA cloning into pUDP002
18516	dg_YCL049C_gRNA	TGTCTCTGACTGTATCTGGA	Diagnostic primer gRNA YCL049C
18521	dg_YCL036W_gRNA	GCGACTCCTCAATGATCAAA	Diagnostic primer gRNA YCL036W
18526	dg_YCL012C_gRNA	CGTCAATATAACTACATTTTGGGA	Diagnostic primer gRNA YCL012C
18531	dg_YCR051W_gRNA	ATACCCCGTTGCACCATG	Diagnostic primer gRNA YCR051W
18536	dg_YCR087C-A_gRNA	CACGCCATCTTCAAACGTCT	Diagnostic primer gRNA YCR087C-A
19067	dg_site1v2_gRNA	CGTATAGCACTCCTGCCGAA	Diagnostic primer gRNA Site 1
19068	dg_site2v2_gRNA	ACTACCCCTAGCACTGCTCA	Diagnostic primer gRNA Site 2
18551	dg_site3_gRNA	GTCGAGAAGATTTCCTGAAGATA	Diagnostic primer gRNA Site 3
18556	dg_site4_gRNA	CGTCATAATGAACAATCTCCAGTG	Diagnostic primer gRNA Site 4
1153	GPDp FW	GACCCACGCATGTATCTATCTC	Diagnostic primer gRNA *Sc*EEB1 & *Sc*EAT1
580	RPXKS1	GAATGTAAGCGTGACATAAC	Diagnostic primer gRNA *Sc*EEB1 & *Sc*EAT1
Construction expression cassettes (ymNeongreen, ymScarletI, *BbALC, LlALDC* and *EaALDC*)			
10320	ConLS_Fw	CATGCGCGGATGACACGAAC	Diagnostic primer YTK
10325	ConR1_Rv	AGTCATCCGAGCGTGTATTG	Diagnostic primer YTK
18759	Bb_aldB-CO-part3_Fw	AAAGCATCGTCTCATCGGTCTCATATGACTACTGCTACTGTTCCAGC	Amplification *BbALDC*
18760	Bb_aldB-CO-part3-Rv	AAAATGCCGTCTCAGGTCTCAGGATAGTTACTTTCTTTCAGATTCAGCTTGGTG	
18761	Ea_ald_CO-part3_Fw	AAAGCATCGTCTCATCGGTCTCATATGAACCACGCTTCTGACTGTAC	Amplification *LlALDC*
18762	Ea_ald_CO-part3-Rv	AAAATGCCGTCTCAGGTCTCAGGATAGTTAAGATTCAACAGATCTGATAGCAG	
18763	Ll_ald_CO-part3-Fw	AAAGCATCGTCTCATCGGTCTCATATGTCTAGATTGTACCAACACGGTAC	Amplification *EaALDC*
18764	Ll_ald_CO-part3-Rv	AAAATGCCGTCTCAGGTCTCAGGATAGTTATTGTTGACCACCTTCAGAAGC	
Construction integration fragments			
18512	ConLS_YCL049C	TTCTATAGATGTACGTAAAGTTCTGCTCTTCTTTTATAGATAAGAGGATTGAGACTCGCCACTGGCCGATAATTGCAGACG	Integration in *Se*YCL049C
18513	ConR1_YCL049C	AGCTCAAGAAAAACCAGGCTATTCGCAGAACAGGATAACCAGCTCTGTAACCACATCAATCATGATGAGCCGTGATGACCC	
18517	ConLS_YCL036W	AGATGCGGCAGCCAGTGAGGGCGTTGGGCATGATCGAAAGCCAAGACCCACCAATTCGAGACTGGCCGATAATTGCAGACG	Integration in *Se*YCL036W
18518	ConR1_YCL036W	ATATACATATACGTACGTATGTATCTACAGAAAGAAAAAAAAAAAAGATCAATGAATATATCATGATGAGCCGTGATGACCC	
18522	ConLS_YCL012C	CAAATTTGAAAGGAACTAAAAAGACAGGAGGAACCTCCCCTTTGTATGAGCTCAAAATAAACTGGCCGATAATTGCAGACG	Integration in *Se*YCL012C
18523	ConR1_YCL012C	CCTCCTCATTCAAGGAAGAGAAATGAAAATACTTCTTGCAAGAAGGTTGCAAATACTATACATGATGAGCCGTGATGACCC	
18527	ConLS_YCR051W	GAGAACAAGAAGAGTTTGCAGGTGACAAAAATCGATGATTATAGGTGTTGTGACGACAAAACTGGCCGATAATTGCAGACG	Integration in *Sc*YCR051W
18528	ConR1_YCR051W	TTCATGTAGCGTCGCGTTCAATTTCTTTTAGCAAGCTATAAGAGCCTTTGTGCTGGGTCGCATGATGAGCCGTGATGACCC	
18532	ConLS_YCR087C-A	AAAAGATGAAACCGAGTAAGCTGCTACATAATGTCTATATATCTACACATAAAATTCCGAACTGGCCGATAATTGCAGACG	Integration in *Sc*YCR087C-A
18533	ConR1_YCR087C-A	TAAGAGTATTCTGTATACAACAGCAAACGGTCTCAGTCAAGAAATATTTGTTATTACAGGCATGATGAGCCGTGATGACCC	
18537	ConLS_Site1	CCTCCGCTATCTAGATGGATACAGAAAGCCGTTTTTTGGTGATTATGTTCACTGTCAAGTACTGGCCGATAATTGCAGACG	Integration in *Se*Site1
18538	ConR1_Site1	CTTAAATTGTGGAAGACTCCATCCAAGAGAAGGATCAGGTATCTGAATTATTCTAAAAGCCATGATGAGCCGTGATGACCC	
18542	ConLS_Site2	ACTCGATGACTCACAGGACAGGAGCGCTTTAAACAAGACGGAATACATAAGCGCATGTGCACTGGCCGATAATTGCAGACG	Integration in *Se*Site2
18543	ConR1_Site2	AAATTACTTCTTGTCATTATAAAAAGACTAGTACGCTTCTATACGTATATTTATTCTCTACATGATGAGCCGTGATGACCC	
18547	ConLS_Site3	AAAGCACACGCTGATTGGTTATATGACACCCAATGGTAAAAGTAAGGTTCAGAACATTAAACTGGCCGATAATTGCAGACG	Integration in *Se*Site3
18548	ConR1_Site3	ATATCTCTTAGGCCAGAATATGTTATTTAACCGTTAAAAGCACTTAGAAGATGACAGGGCCATGATGAGCCGTGATGACCC	
18552	ConLS_Site4	CCAATCAGCGTGTGTTTTATATACCTCTCTTATATAATTTAAGAAAGAACTGCTTATTCTACTGGCCGATAATTGCAGACG	Integration in *Se*Site4
18553	ConR1_Site4	TGTTGGTTTTATAAGCGCATTGATTGTTTGTTTGAGAGTCTTAAAGTCAAATAACACCTGCATGATGAGCCGTGATGACCC	
18981	ConLS_*Sc*EEB1	GGTAGAGAAAGTGGATCGGCGGATTGGAAAGCACAGCGTGGGGAGGATGGTAAATAGAGAACTGGCCGATAATTGCAGACG	Integration in *ScEEB1*
18982	ConR1_*Sc*EEB1	TTTTCGGTATTTTTGAAGATTAGCAAAAAGATCAAGATATCAAGTATTTTCATATTTGTCCATGATGAGCCGTGATGACCC	
18985	ConLS_*Sc*EAT1	TGCTGTGTGCGTTGATTTGGGCCTGACACGAGAAGAAAGTGCGTTACGTACATCAAGATTACTGGCCGATAATTGCAGACG	Integration in *ScEAT1*
18986	ConR1_*Sc*EAT1	CCAAGGTCGAGACGTATACAAACTGCAAAATAAAAGGAACCGTGGGAAGAGGGCTTACAACATGATGAGCCGTGATGACCC	
18768	ConR1_SHR-CB-Rv	CGGTCAGATGGGATACAATCTAGATAAGTTGCGCTGTAGCAGCAAGCTGAATAGCGATGCCATGATGAGCCGTGATGACCC	*In vivo* assembly SHR CB flank incorporation
13047	ConLS_fw_CB	GCATCGCTATTCAGCTTGCTGCTACAGCGCAACTTATCTAGATTGTATCCCATCTGACCGGCCGATAATTGCAGACGAAC	
Diagnostic primers for integration verification			
18514	dg_YCL049C_fw	TCAGTTAGAGTGACAGTTGC	Integration in *Se*YCL049C
18515	dg_YCL049C_rv	GTTGTGCGTTTTACGTGC	
18519	dg_YCL036W_fw	TCCGTCAGTATTCGAGGC	Integration in *Se*YCL036W
18520	dg_YCL036W_rv	TCTTGGAACCTATCCTGGC	
18990	dg_YCL012C_2_fw	GGCTCGAATTTTATTGAGTGG	Integration in *Se*YCL012C
18991	dg_YCL012C_2_rv	GGTATCTAAAATGCGTTCAAGG	
18529	dg_YCR051W_fw	CCATTCATTGTTTAAGTTTCGGG	Integration in *Sc*YCR051W
18530	dg_YCR051W_rv	GCTTTTCTTTCACTCTACAACG	
18534	dg_YCR087C-A_fw	GAATACCTCTTCGAAACGTTGAG	Integration in *Sc*YCR087C-A
18535	dg_YCR087C-A_rv	ATGAGTGGACTGGCAGC	
18539	dg_Site1_fw	GGACATGAAAGAGCCCAG	Integration in *Se*Site1
18540	dg_Site1_rv	CTCAAACGCTACAAAGGAAGC	

(*continued on next page*)

Table 3 (*continued*)

Number	Primer name	Sequence (5' -> 3')	Purpose
18544	dg_Site2_fw	CGTTGGAAAGAGTTGTTACTTTCTG	Integration in *Se*Site2
18545	dg_Site2_rv	GCTTTACACTGATATCAAATAGCC	
18549	dg_Site3_fw	GAGGTCAAAATGTTGATAATTAGGAG	Integration in *Se*Site3
18550	dg_Site3_rv	GCATTTGTAATATTTCCAAGCTGC	
18992	dg_Site4_2_fw	GGAATATGTGACTTCGGGC	Integration in *Se*Site4
18993	dg_Site4_2_rv	ACCTAATCAACGTGAAGGC	
15944	dg_*Sc*EEB1_fw	AGTGCCGCTTCGAAATCATC	Integration in *ScEEB1*
15945	dg_*Sc*EEB1_rv	TTCTGCATCTGGTTGCCTAC	
15950	dg_*Sc*EAT1_fw	CTGGGTTGGAACGAAGTTTG	Integration in *ScEAT1*
15951	dg_*Sc*EAT1_rv	ACCGTCATGAGTGTAGTCAG	

d at 20 °C while shaking at 200 rpm. Then, 1 mL of the cell suspension was transferred to 20 mL fresh YPD hyg medium in shake flasks and grown for 3 d. Finally, 1 mL cell suspension was transferred to non-selective YPD medium for optimal fluorescent gene expression. *In vivo* assembly efficiency of ymNeongreen and ymScarlet genes in CBS 1483 was analysed by measuring fluorescence levels in the BD FACSAria™ II SORP Cell Sorter (BD Biosciences, Franklin Lakes, NJ, USA) equipped with 355, 445, 488, 561 and 640 nm lasers and a 70 μm nozzle, and operated with filtered FACSFlow™ software (BD Biosciences). The fluorophore ymScarletI was excited by the 561 nm laser and emission was detected through a 582 nm bandpass filter with a bandwidth of 15 nm. The fluorophore ymNeongreen was excited by the 488 nm laser and emission was detected through a 545 nm bandpass filter with a bandwidth of 30 nm. The cytometer performance was evaluated prior to each experiment by running a CST cycle with CS&T Beads (BD Biosciences) and the drop delay for sorting was determined by running an Auto Drop Delay cycle with Accudrop Beads (BD Biosciences). For each sample, 100,000 events were analysed. Cell morphology was analysed by plotting forward scatter (FSC) against side scatter (SSC) and the appropriate cell size was gated. Gated cells were used to determine the fluorescence intensity of the cells. Gating windows for fluorescence intensity were based on the fluorescence of the cells transformed with solely ymNeongreen or ymScarletI as repair fragment for sole integrations. Cells in the gate ymNeongreen^{+}ymScarlet^{+} were sorted separately on non-selective YPD plates and grown for 5 d. FACS data was analysed using the Flowing Software version 2.5.1 (Turku Centre for Biotechnology, Finland).

Fermentation in septum flasks

Frozen aliquots of CBS 1483, IMI504-IMI508, IMI510–512, IMI483 and IMI485 were inoculated in 20 mL of YPD media in 50 mL Greiner tubes with air vents at 12 ℃ shaking at 200 rpm and transferred to precultures in 100 mL YPD in 500 mL shake flasks grown at 12 ℃ shaking at 200 rpm. Exponentially growing cells were washed and transferred into 100 mL septum bottles containing 60 mL full malt wort at 5.7°P for strains CBS 1483, IMI504-IMI508, IMI510–512 or in full malt wort at 17^{o} P for strains CBS 1483, IMI483 and IMI485 at a starting OD_{660} of 0.2 mL^{-1}. The cultures were incubated at 12 ℃ and at 200 rpm for five (5.7^{o} P) or eight days (17^{o} P) with regular daily sampling to determine cell density, sugar consumption, ethanol production, esters and ketones concentrations throughout the fermentations.

Analytical techniques

Sugars (glucose, fructose, maltose, maltotriose) and ethanol concentrations were measured using HPLC (Agilent Technologies, 1260 HPLC system; Agilent Technologies, Santa-Clara, CA) equipped with a Bio-Rad HPX-42A column (300 × 7.8 mm, 25 μm) (Bio-Rad, Hercules, CA) and an 1260 Refractive Index Detector as previously described in [11]. Vicinal diketone (diacetyl, 2, 3-pentadione) concentrations were measured using static headspace gas chromatography (GC) in a 7890 A Agilent GC (Agilent Technologies) with an electron capture detector on a CP-Sil 8 CB (50 m x 530 μm x 1 μm) capillary column as previously described in [15]. Higher alcohols and esters were analyzed using static headspace gas chromatography (GC) with a flame ionization detector FID (Agilent technologies 7890 A) and a DB-WAXetr capillary column (30 m x 320 μm x 1 μm) as described in [11].

Whole genome sequencing

Yeast genomic DNA of transformants was isolated using QIAGEN Genomic-tip 100/G kit (Qiagen, Hilden, Germany). Genomic DNA concentrations were measured with the BR ds DNA kit (Invitrogen, Carlsbad, CA, USA) using a Qubit 2.0 Fluorometer (Thermo Fisher Scientific). In-house DNA sequencing was performed using the MiSeq System (Illumina, San Diego, CA, USA). Extracted DNA was mechanically sheared to an aimed average size of 550 bp with the M220 ultrasonicator (Covaris, Wolburn, MA, USA). DNA libraries were prepared using the TruSeq DNA PCR-Free Library Preparation Kit (Illumina) according to the manufacturer's manual. Quantification of the libraries was performed by qPCR using the KAPA Library Quantification Kit for Illumina platforms (Kapa Biosystems, Wilmington, MA, USA) on a Rotor-Gene Q PCR cycler (Qiagen). The library quality was verified on the TapeStation System 4150 (Agilent). All libraries were normalized to 2 nM before the multiplexing step.

All Illumina sequencing (suppl. Table S1) data are available at NCBI (https://www.ncbi.nlm.nih.gov/) under the bioproject accession number PRJNA911296 (study SRP412695). The raw Illumina reads (suppl. Table S1) were aligned against a chromosome-level reference genome of CBS 1483 (NCBI bioproject accession number PRJNA522669, https://www.ncbi.nlm.nih.gov/) [16] using the Burrows–Wheeler Alignment tool (BWA) [34] and further processed with SAMtools [35].

Identification of unique landing sites

Identification of unique landing sites on CHRIII of the CBS 1483 was performed using sequence available at NCBI (https://www.ncbi.nlm.nih.gov/) as bioproject accession numbers PRJNA522669 (Illumina) and PRJNA522669 (Nanopore). The coding sequences and additionally 800 bp upstream and 300 bp downstream were subtracted from the *SeSc*-CHRIII sequence. These non-coding sequences of *SeSc*CHRIII were extracted with bedtools (getfasta option) [36]. The remaining sequence was used to generate *k*-mers with $k = 200$ and $k = 500$ with the ara package (https://github.com/AbeelLab/ara). The resulting *k*-mers were aligned to the CBS 1483 genome using a MUMmer alignment [37] and eliminated upon a match other than its original location in *SeSc*CHRIII. Next, the unique regions were subjected to manual inspection for presence of other essential DNA sequences and discarded when present. Finally, manual screening of the unique landing sites for other essential DNA regions was performed. Genes with non-essential functions as described in the SGD database (https://www.yeastgenome.org/) were selected.

CHRIII configuration analysis

S. pastorianus genomes deposited at NCBI (Bioprojects PRJNA522928 [38], PRJDB4073 [39], PRJNA504476, PRJNA169496) were mapped to the concatenated genome sequences of *S. eubayanus* (CBS 12357) and *S. cerevisiae* (CEN.PK113–7D) using the Burrows-Wheeler Alignment BWA) tool [34] and further process with SAMtools [35]. Coverage of 500 bp window was calculated across the reference and CNV was determined based on Magnolya [40].

Results

Targeting homoeologous genes in CBS 1483 results in unpredictable loss of heterozygosity

To illustrate the unpredictability of the outcome of CRISPR editing in allo-aneuploidy yeast, individual knockout of genes *ScEEB1* and *ScEAT1* was attempted. Sc*EEB1* is carried by *Sc*CHRXVI (two copies) and has a homoeolog (*SeEEB1*) on *Se*CHRXVI (two copies). *ScEAT1* is present on *Sc*CHRVII (one copy) and its homoeolog *SeEAT1* is on *Se*CHRVII (three copies). Deletion of the two copies of Sc*EEB1* in *S. pastorianus* CBS 1483 was performed by co-transforming pUDP168 that expresses a gRNA targeting *ScEEB1* and a repair fragment containing the ymNeongreen

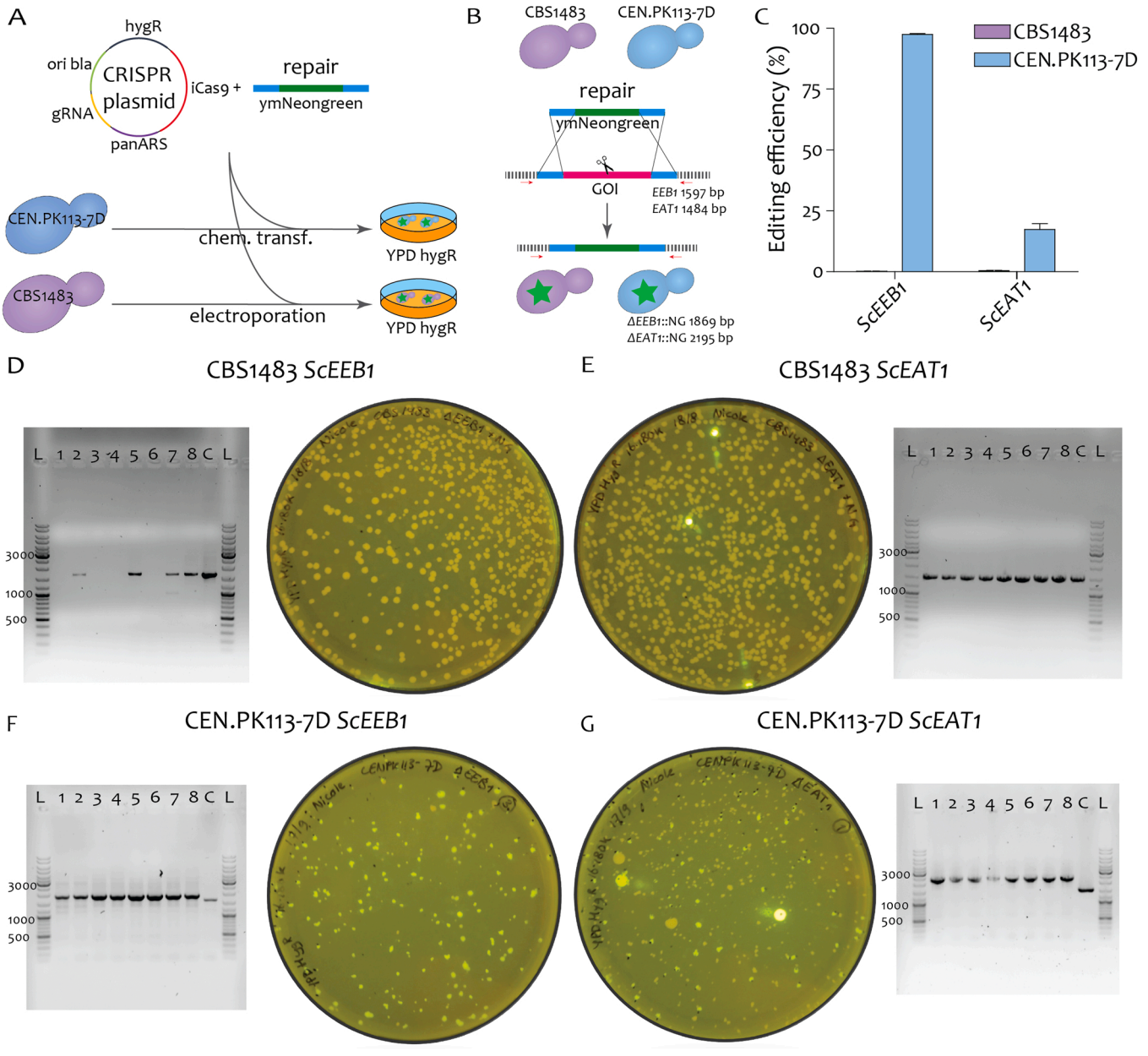

Fig. 1. Genome editing in haploid *S. cerevisiae* CEN.PK113–7D and aneuploidy *S. pastorianus* CBS 1483. A) Schematic representation of the transformation setup and genomic modification. B) Genome editing efficiencies in *S. pastorianus* CBS 1483 (purple bars) and *S. cerevisiae* CEN.PK113–7D (blue bars) targeting the *S. cerevisiae* allele (CBS 1483) or gene (CEN.PK113–7D) *ScEEB1* and *ScEAT1* thereby aiming for ymNeongreen integration. Editing efficiencies were calculated based on number of green fluorescent colonies over the total number of colonies on the transformation plates. Values are derived from three individual transformations. Transformation plates and genotyping of transformants of ymNeongreen integration in *ScEEB1* in *S. pastorianus* CBS 1483 (C), *ScEEB1* in *S. cerevisiae* CEN.PK113–7D (D), *ScEAT1* in *S. pastorianus* CBS 1483 (E) and *ScEAT1* in *S. cerevisiae* CEN.PK113–7D (F). Integration of ymNeongreen results in green fluorescent colonies. Genotyping confirmed integration of ymNeongreen in *ScEEB1* and *ScEAT1* in *S. cerevisiae* CEN.PK113–7D, but not in *S. pastorianus* CBS 1483.

flanked by 60 bp nucleotides homologous to upstream and downstream the *ScEEB1* open reading frame. Similarly deletion of *ScEAT1* was performed using pUDP172 and a ymNeongreen containing repair targeting the *ScEAT1* locus (Fig. 1A-B). Integration of ymNeongreen at the target site resulted in green fluorescent colonies when excited by blue light (Fig. 1A-B). Despite the previously shown successful editing (>90%) of *SeILV6*, *SeATF1* and *SeATF2* in CBS 1483 with CRISPR-Cas9 [26], integration of the ymNeongreen marker at *ScEEB1* or *ScEAT1* loci yielded 0.19% and 0.48% targeting efficiencies, respectively (Fig. 1C). Even though fluorescent transformants were observed, none of them showed the right genotype (Fig. 1D-E).

To eliminate the possible weak activity of the gRNA to programme Cas9 targeting at both sites, the same two deletions were also performed in the haploid *S. cerevisiae* CEN.PK113–7D. Contrasting with the poor efficiency observed in CBS 1483, all CEN.PK113–7D fluorescent transformants tested harbored the correct deletion (Fig. 1C-F-G). However, we observed a clear difference in targeting efficiency between the *ScEEB1* (100%) and *ScEAT1* (20%) editing events (Fig. 1C). This might have been caused by lower spacer efficiency; even though the spacer design included folding analysis to mitigitate occurrence of secondary structures, these events that might hinder target recognition could not be entirely eliminated. Additionally, DNA conformation at the spacer location such as nucleosome positioning, could also affect the editing efficiency; however no further work to elucidate this phenomenon was attempted.

Assuming that the Cas9 guided by the respective gRNAs introduced the DSB successfully, the remaining question was how does *S. pastorianus* repair the DSB event that, if not repaired, is lethal for the cell. To elucidate this mechanism, four non fluorescent transformants from *ScEEB1* deletion transformation were randomly selected and subjected to whole genome sequencing (WGS).

Sequencing analysis confirmed that transformants had failed to incorporate the supplied repair fragment, but instead repaired the DSB with the homoeologous *S. eubayanus* CHRXVI as template for HDR, resulting in loss of heterozygosity (Fig. 2, suppl. Fig. S1, suppl. Table S1). Each transformant exhibited a different pattern: colony 1 (IMK1062), colony 4 (IMK1064) and colony 3 (IMK1063) were repaired by a 5 kbp, 10 kbp and 26-kbp region surrounding the *ScEEB1* gene, respectively, while in colony 6 (IMK1065) over 700 kbp from the *Sc*CHRXVI was replaced by the homologous sequence from the *Se*CHRXVI sequence and only the subtelomeric regions of *Sc*CHRXVI were retained (Fig. 2, suppl. Fig. S1, suppl. Table S1). Therefore, loss of heterozygosity resulting from preferential usage of the homoeologous chromosome is an undesired side-effect of Cas9-mediated genome editing and has a major impact on the editing specificity and efficiency in allo-aneuploid yeasts, including *S. pastorianus* CBS 1483.

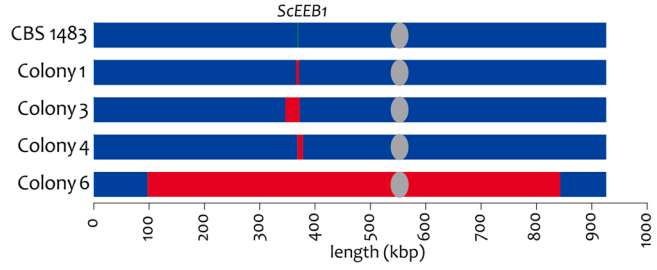

Fig. 2. Whole genome sequencing reveals that CRISPR-Cas9 editing in the allo-aneuploid yeast *S. pastorianus* CBS 1483 aiming to integrate ymNeongreen in *ScEEB1* on *Sc*CHXVI results in loss of heterozygosity in all four colonies tested. The red and blue color indicate chromosome assigned as *S. eubayanus* and *S. cerevisiae* respectively.

A systematic strategy to identify unique landing sites for CRISPR-Cas9 targeting

Genome editing with CRISPR-Cas9 allows gene deletions, gene integrations and gene modifications to be made. In the case of gene deletions and gene modifications, the user is restricted to the location of the gene of interest in the genome. On the other hand, additional genes can be integrated at any user-chosen genomic location. Therefore, identification of chromosomal regions (landing sites) devoid of homoeologous regions for gene integrations with CRISPR-Cas9 in the allo-aneuploid yeast strain *S. pastorianus* CBS 1483 would be of a prime importance. Landing sites should meet the following criteria: (i) the frequency for LOH is low, (ii) the gRNA targets the protospacer with high efficiency, and (iii) gene integration does not result in undesired changes in the cell's physiology.

To prevent unwanted repairs that would use the homoeologous chromosome, the search for landing sites was first limited to the chimeric *SeSc*CHRIII, that is composed of two-thirds from the *S. eubayanus* parent and one-third from *S. cerevisiae,* and is characterized by the absence of homoelogous sequence [15,16]. First, a systematic approach to finding suitable integration sites on *SeSc*CHRIII was developed. Since modification at a landing site should remain metabolically neutral, i.e. should not impact yeast physiology, coding sequences including 800 bp upstream and 300 bp downstream covering the promoter and terminator regions were subtracted from the *SeSc*-CHRIII sequence. This thorough *in silico* analysis revealed a set of 23 non-coding regions (total of 34.7 kbp) ranging from 30 bp to more than 6 kbp (Fig. 3, suppl. Table S2). These non-coding sequences were used to generate *k*-mers of 100, 150, 200, 300 and 500 nucleotides which were aligned to CBS 1483 genome using MUMmer [37]. *K*-mers with small, partial alignments to other chromosomes were discarded to avoid selection of sequences containing homology with other parts of the genome and only *k*-mers that returned one hit located on *SeSc*CHRIII were selected. This resulted in a total of 283 and 50 unique *k*-mers for respectively $k = 200$ and $k = 500$, residing in a total of 26 regions (total 22.4 kbp, average length of 863 bp) and 17 regions (total 23.9 kbp, average length of 1403 bp), respectively. Since unique *k*-mers could be adjacent and overlap one another, the 17 unique regions of the $k = 500$ output were identified spanning lengths from 198 to 3213 bp. These 17 unique regions were manually checked for the presence of other essential DNA regions, such as tRNAs, telomeres, centromeres and autonomous replication sequences. Out of the 13 regions that passed the final check, four landing sites distributed over *SeSc*CHRIII, referred to as Sites 1, 2, 3 and 4, were chosen to investigate their potential use for genomic integrations in CBS 1483. Secondly, a manual screening of *SeSc*CHRIII for non-essential genes was deployed to find landing sites located in gene encoding regions. The search resulted in 13 genes suitable as landing sites (suppl. Table S3) of which the following five genes distributed over the chromosome were selected: *Se*YCL049C, *Se*YCL036W, *Se*YCL012C, *Sc*YCR051W and *Sc*YCR087C-A. In total, nine genes and sites were retained as potential landing sites on CBS 1483 *SeSc*CHRIII (Table 4, Fig. 3).

CRISPR-Cas9 targeting of unique landing sites allows efficient gene integration

To evaluate the landing sites for genomic integrations, gRNAs for all landing sites were designed considering GC-content, secondary structure, off-targets and allelic variation that may occur within the four copies of the CBS 1483 chimeric *SeSc*CHRIII (suppl. Table S4). To evaluate the CRISPR-editing in the 9 selected landing sites, the CRISPR-plasmid co-expressing *Streptococcus pyogenes* iCas9^{D147Y,P411T} and the respective gRNA [30] were co-transformed with the ymNeongreen repair fragment, allowing visual screening of edited colonies, into CBS 1483.

Targeting the landing sites *SeYLC049C*, *Se*YCL036W, *Se*YCL012C,

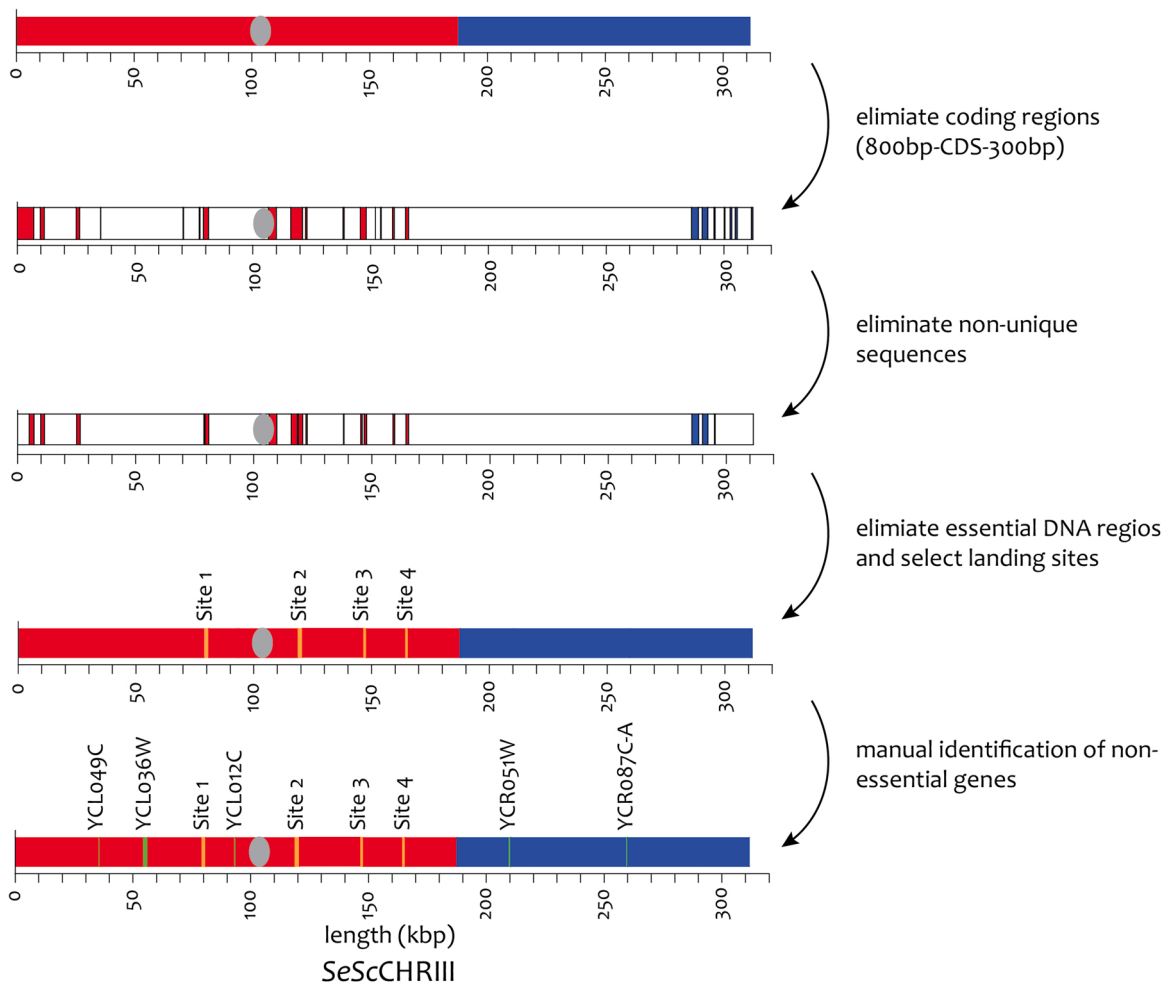

Fig. 3. Strategy to identify non-coding unique DNA sequences in CBS 1483 *Se*Sc*c*HRIII. In the first step, non-coding regions were obtained by subtracting the coding sequences plus 800 bp upstream and 300 bp downstream covering for promoter and terminator regions. In the second step, the unique regions were obtained by selecting unique *k*-mers when aligning to the CBS 1483 genome and the non-unique sequences were eliminated. In the next step, the non-coding unique sequences were checked for the presence of essential DNA regions. Additionally, potential landing sites identified by manual screening of non-essential genes were selected, resulting in a total of nine landing sites.

Table 4
Overview of the selected landing sites on *Se*Sc*c*HRIII in *S. pastorianus* CBS 1483.

Landing site	Start coordinate	Stop coordinate	Strand	Size (bp)
YCL049C	35643	35915	-	884
YCL036W	54552	56237	+	1685
Site 1	79419	80823	n.a.	1404
YCL012C	93151	93617	-	466
Site 2	118822	120628	n.a.	1806
Site 3	146704	147799	n.a.	1095
Site 4	164540	165542	n.a.	1002
YCR051W	209678	210346	+	668
YCR087C-A	259551	259985	-	434

n.a. Not Applicable

*Sc*YCR051W, *Sc*YCR087C-A, *Se*Site2, *Se*Site3 and *Se*Site4 resulted in high editing efficiencies, which is reflected in the number of green fluorescent colonies on the transformation plates (Fig. 4). Genotyping of 10 colonies for each landing site showed 100% correct ymNeongreen integration in *Se*YCL049C, *Se*YCL012C, *Sc*YCR051W, *Sc*YCR087C-A, *Se*Site2, *Se*Site3 and *Se*Site4 (suppl. Fig. S2). Genotyping of *Se*YCL036W showed that 11 out of the 12 assessed colonies were correctly edited and showed correct integration of the ymNeongreen expression cassette (suppl. Fig. S3). Only integration at *Se*Site1 did not result in high editing efficiencies, possibly due to the low gRNA efficiency (Fig. 4). Thus, 8 out of 9 identified landing sites showed high potential for standard genomic integrations in *S. pastorianus* CBS 1483 as they were targeted with high efficiency and do not cause loss of heterozygosity.

Some of the landing sites can be used in multiple S. pastorianus strains: the example of Weihenstephan 34/70

The use of these integration sites is not just restricted to the CBS 1483 strain. Genome-wide analysis of different *S. pastorianus* genomes deposited at NCBI (https://www.ncbi.nlm.nih.gov/), revealed that the large majority of the strains (45 out of 47 strains) harbors the chimeric *Se*Sc*c*HRIII in various copy numbers, either as sole CHRIII configuration (two strains) or in combination with *Sc*CHRIII (39 strains) or *Se*CHRIII (four strains) (Fig. 5A). In any configuration, the entire *Se*Sc*c*HRIII, if present alone as in CBS1483 or part of it, is unique. This is exemplified by the *S. pastorianus* WS 34/70 strain, which counts 3 copies of the chimeric *Se*Sc*c*HRIII and one full length copy of the *Sc*CHRIII (Fig. 5B). Whereas the sequence similarity of the shared *Sc*CHRIII part is close to 100%, the sequence homology between the *Se*CHRIII part and the *Sc*CHRIII part is only 80–85%. In this genome configuration, this means that only the distal *S. cerevisiae* sequence of *Se*Sc*c*HRIII including the *Sc*YCR051W and *Sc*YCR087C-A sites could lead to efficient editing. To test this hypothesis, the WS 34/70 strain was transformed with the gRNA expressing plasmids targeting the 8 most efficient landing sites

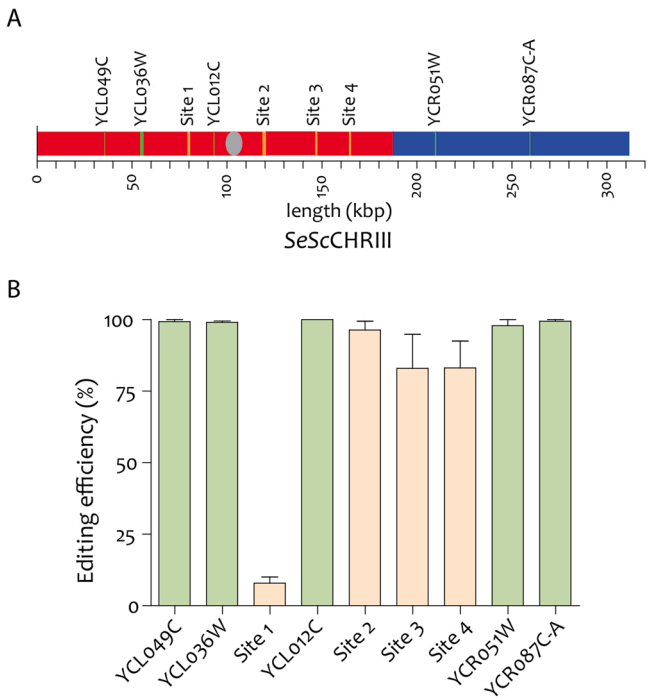

Fig. 4. A) Overview of the identified landing sites in CBS 1483. B) Genome editing efficiencies in *S. pastorianus* CBS 1483 targeting the identified landing sites on *Se*Sc*CHRIII thereby aiming for ymNeongreen integration. Editing efficiencies were calculated based on number of green fluorescent colonies over the total number of colonies on the transformation plates. Values are derived from three individual transformations.

previously identified and their respective repair DNA containing the fluorescent marker. The integration sites lacking homoeologous sequences, *Sc*YCR051W or *Sc*YCR087C-A, showed, as anticipated, a high targeting efficiency exceeding 50% (Fig. 5B). For the proximal landing sites *Se*YCL049C, *Se*YCL036W, *Se*YCL012C and *Se*Site2, there was a significant drop in efficiency (<50%). Remarkably, the efficiency of the editing at *Se*Site3 and *Se*Site4 was to a lesser extent not hampered by the presence of the *S. cerevisiae* sequence, contrasting with results at other chromosomal sites indicating that other genetic factors might play a role.

Genomic integrations at landing sites do not result in changes in physiology and brewing characteristics

One of the criteria for a good landing site is that integration of DNA at this location should not have a physiological effect on the cell compared to the parental CBS 1483 strain. To investigate potential physiological effect on genomic integrations, the strains CBS 1483 and IMI504–8 and IMI510–512 containing ymNeongreen in their respective landing sites, were cultivated in septum flasks under brewing conditions (full malt wort at 5.7° P and at 12 °C). Deviations in growth, sugar consumption, flavor molecule production and ethanol production were evaluated relative to the parental strain CBS 1483 (Fig. 6). Early in the fermentation, the deviations in produced metabolites (e.g. glycerol (0.013 ± 0.033 g L^{-1} for CBS 1483 and 0.000 ± 0.000 g L^{-1} for all other strains, compared to > 0.700 g L^{-1} respective end concentrations) and ethyl acetate (0.147 ± 0.127 mg L^{-1} for CBS 1483 and 0.000 ± 0.000 mg L^{-1} for six other strains, compared to > 1.100 mg L^{-1} respective end concentrations)) can have large effects on the fold change, but represent only a very small fraction of the final concentrations. Integration in the landing sites *Se*YCL049C, *Se*YCL036W, *Se*YCL012C, *Sc*YCR051W, *Sc*YCR087C-A, *Se*Site2 and *Se*Site3 did not have a significant effect on the physiological behaviour of the strain and are therefore suited for gene integrations. In contrast, IMI512 (site4::ymNeongreen) showed slower growth as well as slower sugar consumption and ethanol production compared to the parental strain CBS 1483. Also, the production of vicinal diketones and esters that contribute to beer flavor was lower for ethyl acetate, isoamyl alcohol, isoamyl ester and isobutanol, whereas the production of ethyl butyrate was higher compared to CBS 1483 after 6 days of cultivation. These observations would suggest that *Se*Site4 would be less suitable for integration of genes of interest. However, although genotyping of the ymNeongreen integration at the *Se*site4 predicted a correct integration, it could not be excluded that other unintended modifications occurred during the transformation (e.g. alteration of chromosome copy number) since the tested transformant was not whole genome sequenced [19].

Integration of acetolactate decarboxylase to eliminate diacetyl production

To demonstrate the reliability of the selected sites, lager brewing yeast strains with reduced diacetyl production were constructed. The vicinal diketone diacetyl is one of the main off-flavors in lager-style beers. The lagering period after the fermentation is required for the reduction of diacetyl and has a major impact on the time and energy of the brewing process. Diacetyl is formed in the supernatant by spontaneous decarboxylation from excreted α-acetolactate, an intermediate of valine and leucine biosynthesis. During the lagering, the brewing yeast reduces diacetyl sequentially to acetoin and 2,3 butanediol [41,42].

To prevent α-acetolactate leakage, an α-acetolactate decarboxylase (AldC), that catalyzes the decarboxylation of α-acetolactate to acetoin, can be expressed. α-*aldC* genes of prokaryotic origin have already been successfully expressed in brewing yeasts, including *S. cerevisiae* [43,44], *S. uvarum* [44,45], *S. carlsbergensis* [46] and *S. pastorianus* [47] have shown great reduction in diacetyl formation resulting in significant shortening of the lagering. Two different *α-aldC* genes were chosen, originating from *Brevibacillus brevis* (*BbaldC*) and *Leuconostoc lactis* (*LlaldC*). To ensure high gene expression levels, the genes were placed under control of the constitutive Sc*PGK1* promoter [48] and the Sc*ADH1* terminator. Linear fragments containing the expression cassettes with 60 bp homologous flanks were co-transformed with the CRISPR-plasmid pUDP273 targeting the landing site YCR087C-A into CBS 1483. The transformation efficiency, calculated based on the percentage of positive colonies verified by diagnostic PCR, was 100% and 79% for *BbaldC* and *LlaldC*, respectively (suppl. Table S6). The correctly edited transformants were named IMI483 *(BbaldC)* and IMI485 *(LlaldC)*.

The strains IMI483 (*BbaldC*) and IMI485 (*LlaldC*), were assessed for diacetyl production in septum flask cultivation on 17 °P full malt wort at 12 °C and compared to CBS 1483. In agreement with previous results [42–46,49–51], heterologous expression of an α-*aldC* gene in CBS 1483 likely eliminated the diffusion of α-acetolactate into the extracellular space preventing formation of diacetyl and therefore the need of its reduction (Fig. 7). Nonetheless, the growth of IMI485 was hampered compared to the parental strain CBS 1483, caused by loss of the ability to consume maltotriose (suppl. Fig. S4). As previously reported for *Se*Site4, despite correct integration, specific transformants might exhibit altered performances probably caused by unintended genetic alterations. Although, this case showed that the landing sites identified for *S. pastorianus* CBS 1483 were suitable for efficient and reliable engineering requiring CRISPR-Cas9 guided integration, a more extensive geno- and phenotyping characterization would be required to select engineered strains retaining all essential brewing traits.

Successful genomic integration through in vivo assembly into ScSeCHRIII landing sites

One of the startling genetic characteristics of *S. cerevisiae* is its ability to recombine multiple linear DNA fragments at a single chromosomal locus. This is often referred to as *in vivo* DNA assembly. We demonstrated that elimination of competing mechanisms, using the homoeologous

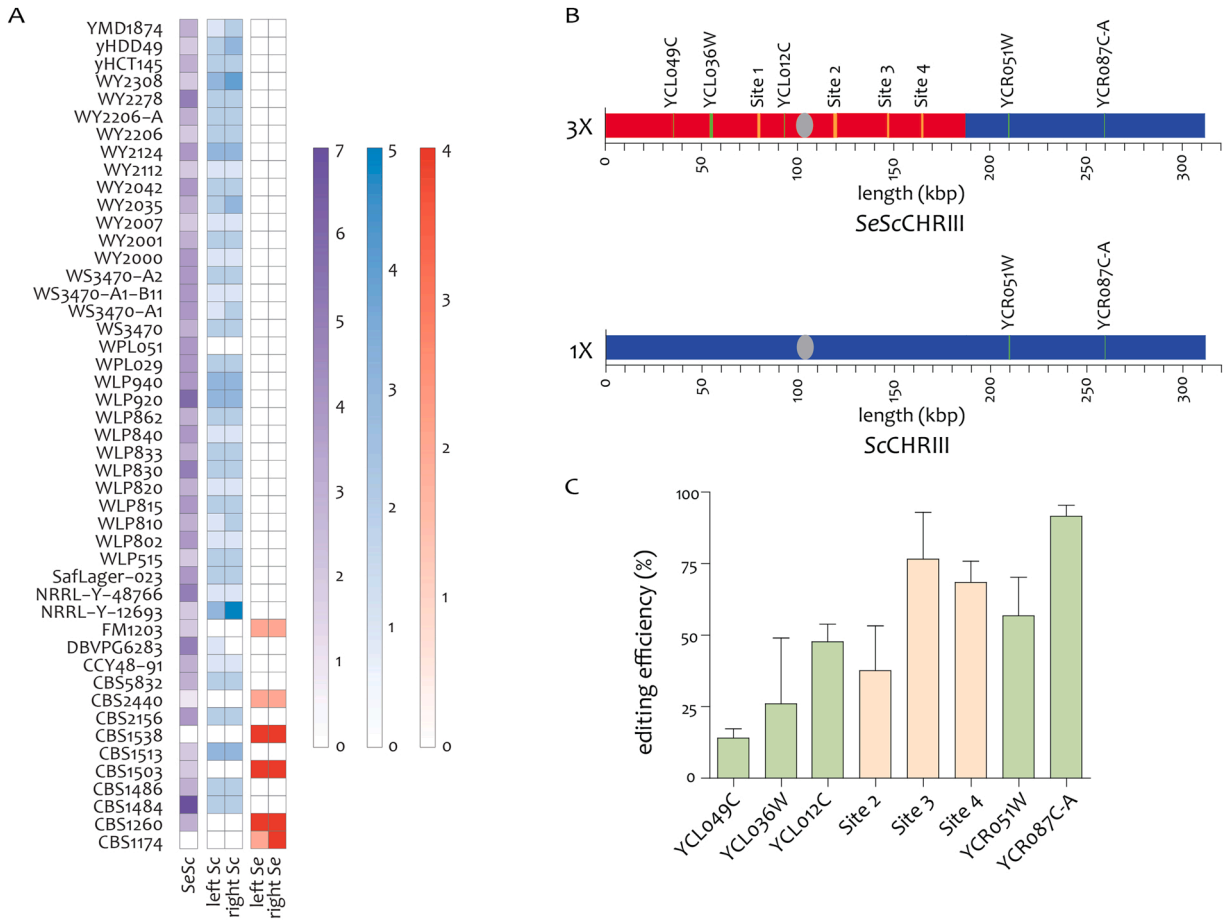

Fig. 5. A) Overview of CHRIII genetic configurations in 47 different *S. pastorianus* strains. B) Chromosome III configurations in *S. pastorianus* WS 34/70. In comparison to CBS 1483, WS 34/70 has an additional *Sc*CHRIII and one less hybrid *SeSc*CHRIII. C) Genome editing efficiencies in *S. pastorianus* WS 34/70 targeting the identified landing sites thereby aiming for ymNeongreen integration. Editing efficiencies were calculated based on number of green fluorescent colonies over the total number of colonies on the transformation plates. Values are derived from three individual transformations.

chromosome as template, improved targeting efficiency of repair fragment integration at chosen chromosomal sites. To investigate the possibility to integrate two fragments simultaneously by HDR, *S. pastorianus* CBS 1483 was co-transformed with pUDP269, a plasmid that expresses a gRNA targeting the *Se*YCL049C landing site and two DNA repair fragments. The first DNA fragment consisted of the ymNeongreen expression cassette that was flanked by 60 bp homologous region upstream to the *Se*YCL049C genomic locus and 60 bp SHR sequences [52], whereas the second fragment encoded the ymScarletI gene flanked by 60 bp SHR sequence complementary to that of the first fragment and 60 bp homologous flanks downstream the *Se*YCL049C landing site. The use of fluorescent genes for the integration allowed for screening of the transformed cell population by Fluorescence-Activated Cell Sorting. Screening of the transformant population revealed that 17.67 ± 1.98% of the transformed cells harbored both fluorescent markers (suppl. Fig. S5). To confirm that the fluorescence was well derived from single and not aggregated cells, for this, single cells from the ymNeongreen^{+} ymScarletI^{+} gated population were sorted on non-selective medium (suppl. Fig. S5). Cultivation of the sorted single cells and subsequent flow cytometry analysis of 12 clones confirmed co-occurrence of both ymNeongreen and ymScarletI fluorescence (suppl.Fig. S6). Genotyping revealed, in all 12 screened colonies, correct integration of both genes in the *Se*YCL049C landing site (Fig. 8). These results showed that genomic integration of *in vivo* assembled DNA fragments is also possible in the interspecific hybrid *S. pastorianus*.

Discussion

CRISPR-mediated gene editing in diploid and more generally polyploid heterozygous yeasts is drastically impaired when not all chromosomes are simultaneously targeted by a programmed CRISPR endonuclease. In such conditions, the still intact homologous chromosome is used as preferential template to fix the double strand break by homology-directed repair. This resolution of the introduced cut can result in chromosome recombinations, which can lead to loss of heterozygosity [20,53,54]. LOH competes with an intended gene-editing repair event and results in reduced editing efficiencies and possibly in extensive genetic changes. In this study, it was demonstrated that this mechanism could also occur between homoeologous chromosomes in the interspecific hybrid yeast *S. pastorianus*. While in diploid yeasts the problem might be restricted to a few heterozygous locations, and easily solved by designing guide-RNA targeting all chromosomes, in *S. pastorianus,* an interspecific hybrid that retained the quasi complete parental genomes, the problem is extended to every single nucleotide since any edit on the chromosome of one of the sub-genome *e.g. S. cerevisiae*, can be repaired with its homoeologous counterpart *e.g. S. eubayanus*. As observed in this study, whether repaired by the donor repair DNA or by the homoeologous chromosome, the resulting chromosomal locus was converted identically in all copies, suggesting that the first repaired site preferentially converts the other. This unpredictability, unfortunately, affects the progress of functional genetic studies in hybrid, industrial yeasts, since the introduction of accurate genetic alterations would have to rely on HDR without introduction of a DSB

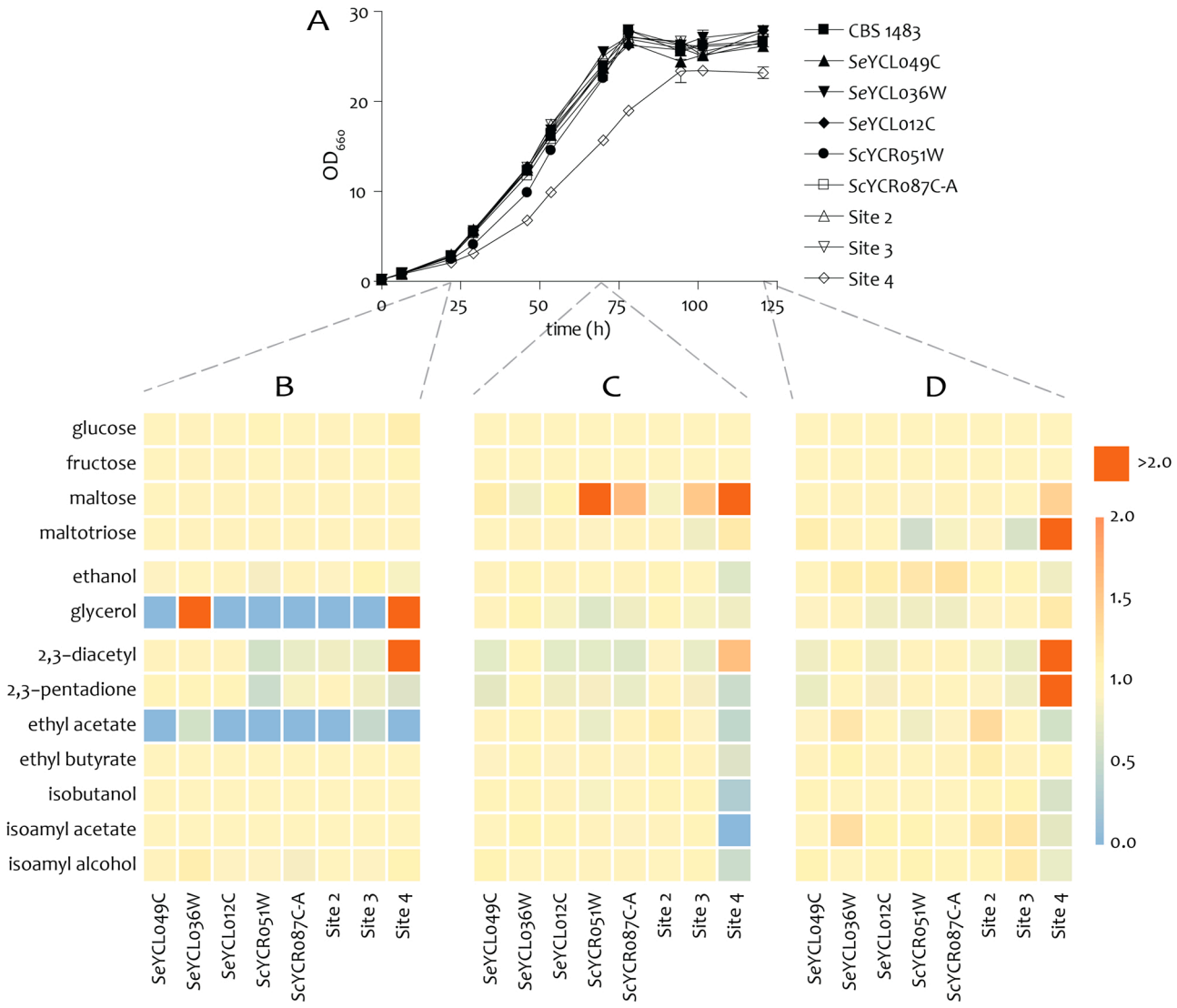

Fig. 6. Physiological characterization of landing site disruptions under brewing conditions. A) Growth curves as function of OD660nm of the *S. pastorianus* strain CBS1483 and derived strains IMI504 (Δ*Se*YCL049C), IMI505 (Δ*Se*YCL036W), IMI506 (Δ*Se*YCL012C), IMI507 (Δ*Sc*YCR051W), IMI508 (Δ*Sc*YCR087C-A), IMI509 (Δ*Se*Site1), IMI510 (Δ*Se*Site2), IMI511 (Δ*Se*Site3), IMI512 (Δ*Se*Site4) harboring a ymNeongreen expression cassettes inserted at single landing sites grown in septum flasks under brewing conditions with full malt wort (5.7° P) at 12 °C. The values represent averages ± mean deviations of data obtained from independent triplicate cultures. At B) t_{19}, C) t_{68} and D) t_{116} hours supernatant samples were analysed for extracellular sugars (glucose, fructose, maltose, maltotriose), ethanol, glycerol, vicinal diketones (diacetyl, 2, 3-pentadione), higher alcohols (isoamyl alcohol, isobutanol) and ethyl (ethyl acetate, ethyl butyrate) and acetate (isoamyl acetate) esters. Concentrations relative to the reference strain CBS 1483 are represented in heatmaps and fold-change in concentrations are color-coded according the scale provided right to heatmap D).

[55,56], methods that require the use of selectable markers and are iterative in nature, since it can replace one allele at the time (e.g. deletion of a gene carried by a trisomic chromosome will require three rounds of transformations) [57,58]. Therefore, improving the predictability of the editing event is critical to enable efficient gene deletion or *in vivo* site-directed mutagenesis.

Genome-wide analysis of different *S. pastorianus* genomes deposited at NCBI (https://www.ncbi.nlm.nih.gov/) showed that chimeric *SeSc*-CHRIII chromosome was nearly always present (found in 45 out of the 47 *S. pastorianus* genomes analysed (Fig. 5A)) as sole CHRIII or in combination with either a *Se*CHRII or *Sc*CHRIII version. In any configuration, the entire CHRIII or part of it is unique. In contrast to targeted sites on other chromosomes, the targeting efficiency of the site on *SeSc*CHRIII region devoid of homoeologous sequences was high and reached up to 100% in some instances. Refuting previous statements, these results demonstrated that homologous recombination was not impaired in *S. pastorianus* but was instead masked. It could also be excluded that genome complexity, increased ploidy and chromosome copy number were also not hindering efficient repair of DSB, as *S. pastorianus* CBS 1483 could efficiently repair tetrasomic *SeSc*CHRIII. CRISPR-Cas9 mediated *in vivo* recombination of two DNA fragments further confirmed that, at selected loci, *S. pastorianus* could perform elaborated homology directed repair with high efficiency. Improving the targeting efficiency in lager brewing yeasts, provides new opportunities to accurately and time-effectively engineer *S. pastorianus* strains with new characteristics. Such strategies could swiftly and efficiently improve a wide range of phenotypic traits and fermentation characteristics, including wort sugar utilization, fermentation rate and energetic performance [6,11], reduction of off-flavor [47,58] and balanced flavor profiles and, moreover, engineering of novel flavors [59,60].

It remains however important to evaluate the targeted integration on the genetic level and screen multiple colonies on phenotype to avoid loss of relevant characteristics resulting from secondary effects. It is indeed known that transformation procedures are mutagenic and in such

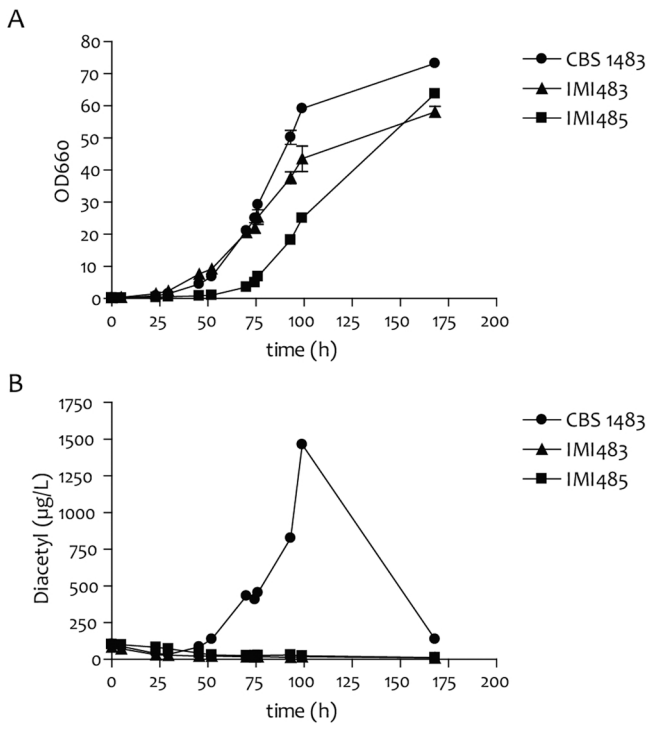

Fig. 7. Performance of CBS 1483 strains expressing different prokaryotic *aldC* genes. A) Growth curve and B) diacetyl concentration of CBS 1483 (•), IMI483 (expressing *BbaldC*, ▲) and IMI485 (expressing *LlaldC*, ■) grown on full malt wort (17°P, 12 °C). The values represent averages ± mean deviations of data obtained from independent triplicate cultures.

aneuploid organisms may lead to chromosome copy number variations that could impact other phenotypic traits unintentionally [15,19]. To completely eliminate this possibility, systematic genome sequencing of engineered strains could be implemented.

Even though *S. pastorianus* is the most industrially used interspecific hybrid between *Saccharomyces* species yeasts, numerous independently formed natural hybrids between *Saccharomyces* species (e.g. *S. cerevisiae* X *S. kudriavzevii*, *S. cerevisiae* X *S. eubayanus* and *S. cerevisiae* X *S. kudriavzevii* X *S. eubayanus*) have been isolated from wine, beer, or cider fermentations [61–66]. Natural interspecific hybrids are not limited to the *Saccharomyces* species group. Several examples have also been described in *Zygosaccharomyces* [67] and *Millerozyma* [68]. Often, these hybrids exhibit better characteristics in fermentation processes than the parental strains, as this heterosis provides a competitive advantage by enabling transgressive phenotypes in man-made environments, and also drives adaptation and fungal evolution. The guiding principles presented in this study should also be helpful to dissecting the genetic background of heterosis in yeast hybrids other than *S. pastorianus* and contribute to engineering these yeasts in the future.

Funding

This work was performed within the Top consortia for Knowledge and Innovation (TKIs) AgriFood which was granted a PPP allowance from the Ministry of Economic Affairs and Climate Policy (Project Habitats #PPPS1701).

CRediT authorship contribution statement

JMGD and NXB designed experiments. MK executed the diacetyl study, NXB executed all other experiments. NXB and MvdB performed bioinformatics analysis. NXB and JMGD supervised the study. NXB and JMGD wrote the manuscript. All authors read and approved the final manuscript.

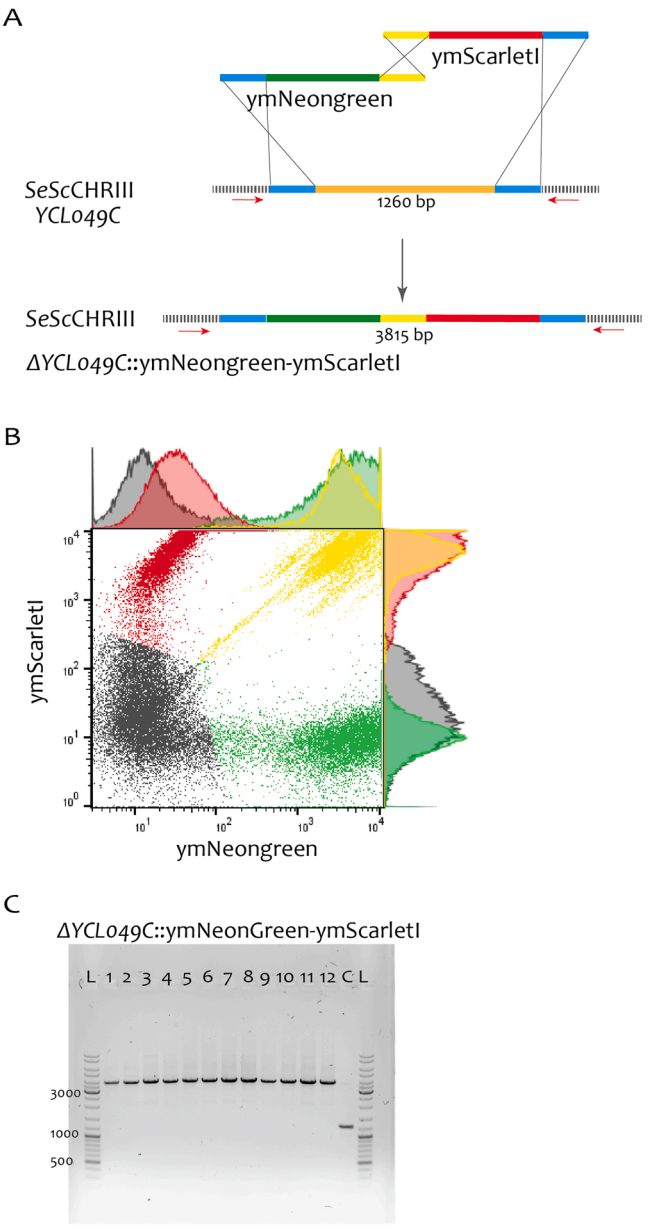

Fig. 8. Genomic integration into landing site *SeYCL049C* of two in vivo assembled DNA fragments expressing ymNeongreen and ScarletI. A) Schematic overview of the genomic integration strategy for in vivo assembly of ymNeongreen and ScarletI DNA fragments. B) Fluorescent profile the transformed population when aiming for integration of two fluorescent expression cassettes. The fluorescence corresponding to ymNeongreen and ymScarlet is plotted for 100,000 events. Flow cytometry was performed for three biological replicates; one representative replicate is shown. C) Genotyping of the sorted ymNeongreen^{+}Scarlet^{+} single colony isolates.

Declaration of Competing Interest

The authors declare that they have no known competing financial interests or personal relationships that could have appeared to influence the work reported in this paper.

Data Availability

Data underlying graphs and figures found in this manuscript are deposited at the 4TU research dat center (https://data.4tu.nl/) and

available through the doi: 10.4121/21648329.

Acknowledgments

We thank Sofia Dashko for cloning plasmid pGGKd034 and Sasha Yogiswara for cloning pUDP168 and pUDP172. We are thankful to Prof. J.T. Pronk (Delft University of Technology), Dr. V.M. Boer and Mr. T. Elink Schuurman (HEINEKEN Supply Chain B.V.) for their support during this project.

Appendix A. Supporting information

Supplementary data associated with this article can be found in the online version at doi:10.1016/j.nbt.2023.04.001.

References

[1] Nakao Y, Kanamori T, Itoh T, Kodama Y, Rainieri S, Nakamura N, et al. Genome sequence of the lager brewing yeast, an interspecies hybrid. DNA Res 2009;16:115–29. https://doi.org/10.1093/dnares/dsp003.

[2] Libkind D, Hittinger CT, Valério E, Gonçalves C, Dover J, Johnston M, et al. Microbe domestication and the identification of the wild genetic stock of lager-brewing yeast. Proc Natl Acad Sci 2011;108:14539–44. https://doi.org/10.1073/pnas.1105430108.

[3] Bergin SA, Allen S, Hession C, Ó Cinnéide E, Ryan A, Byrne KP, et al. Identification of European isolates of the lager yeast parent *Saccharomyces eubayanus*. FEMS Yeast Res 2022;22. https://doi.org/10.1093/femsyr/foac053.

[4] Blieck L, Toye G, Dumortier F, Verstrepen KJ, Delvaux FR, Thevelein JM, et al. Isolation and characterization of brewer's yeast variants with improved fermentation performance under high-gravity conditions. Appl Environ Microbiol 2007;73:815–24. https://doi.org/10.1128/aem.02109-06.

[5] Iattici F, Catallo M, Solieri L. Designing new yeasts for craft brewing: when natural biodiversity meets biotechnology. Beverages 2020;6:3. https://doi.org/10.3390/beverages6010003.

[6] Ekberg J, Rautio J, Mattinen L, Vidgren V, Londesborough J, Gibson BR. Adaptive evolution of the lager brewing yeast *Saccharomyces pastorianus* for improved growth under hyperosmotic conditions and its influence on fermentation performance. FEMS Yeast Res 2013;13:335–49. https://doi.org/10.1111/1567-1364.12038.

[7] Gibson B, Dahabieh M, Krogerus K, Jouhten P, Magalhães F, Pereira R, et al. Adaptive laboratory evolution of ale and lager yeasts for improved brewing efficiency and beer quality. Annu Rev Food Sci Technol 2020;11:23–44. https://doi.org/10.1146/annurev-food-032519-051715.

[8] Gorter de Vries AR, Voskamp MA, van Aalst ACA, Kristensen LH, Jansen L, van den Broek M, et al. Laboratory evolution of a *Saccharomyces cerevisiae* × *S. eubayanus* hybrid under simulated lager-brewing conditions. Front Genet 2019;10:242. https://doi.org/10.3389/fgene.2019.00242.

[9] Steensels J, Snoek T, Meersman E, Picca Nicolino M, Voordeckers K, Verstrepen KJ. Improving industrial yeast strains: exploiting natural and artificial diversity. FEMS Microbiol Rev 2014;38:947–95. https://doi.org/10.1111/1574-6976.12073.

[10] Krogerus K, Magalhães F, Vidgren V, Gibson B. New lager yeast strains generated by interspecific hybridization. J Ind Microbiol Biotechnol 2015;42:769–78. https://doi.org/10.1007/s10295-015-1597-6.

[11] Brickwedde A, van den Broek M, Geertman JA, Magalhães F, Kuijpers NGA, Gibson B, et al. Evolutionary engineering in chemostat cultures for improved maltotriose fermentation kinetics in *Saccharomyces pastorianus* lager brewing yeast. Front Microbiol 2017;8:1690. https://doi.org/10.3389/fmicb.2017.01690.

[12] Gorter de Vries AR, Pronk JT, Daran J-MG. Lager-brewing yeasts in the era of modern genetics. FEMS Yeast Res 2019;19. https://doi.org/10.1093/femsyr/foz063.

[13] Walther A, Hesselbart A, Wendland J. Genome sequence of *Saccharomyces carlsbergensis*, the world's first pure culture lager yeast. G3 Genes|Genomes|Genet 2014;4:783–93. https://doi.org/10.1534/g3.113.010090.

[14] Turgeon Z, Sierocinski T, Brimacombe CA, Jin Y, Goldhawke B, Swanson JM, et al. Industrially applicable *de novo* lager yeast hybrids with a unique genomic architecture: creation and characterization. Appl Environ Microbiol 2021;87. https://doi.org/10.1128/aem.02434-20.

[15] Broek Mvd, Bolat I, Nijkamp JF, Ramos E, Luttik MAH, Koopman F, et al. Chromosomal copy number variation in *Saccharomyces pastorianus* is evidence for extensive genome dynamics in industrial lager brewing strains. Appl Environ Microbiol 2015;81:6253–67. https://doi.org/10.1128/AEM.01263-15.

[16] Salazar AN, Gorter de Vries AR, van den Broek M, Brouwers N, de la Torre Cortès P, Kuijpers NGA, et al. Chromosome level assembly and comparative genome analysis confirm lager-brewing yeasts originated from a single hybridization. BMC Genom 2019;20:916. https://doi.org/10.1186/s12864-019-6263-3.

[17] Glover NM, Redestig H, Dessimoz C. Homoeologs: what are they and how do we infer them? Trends Plant Sci 2016;21:609–21. https://doi.org/10.1016/j.tplants.2016.02.005.

[18] Brouwers N, Brickwedde A, Gorter de Vries AR, van den Broek M, Weening SM, van den Eijnden L, et al. Himalayan *Saccharomyces eubayanus* genome sequences reveal genetic markers explaining heterotic maltotriose consumption by *Saccharomyces pastorianus* hybrids. Applied. Environ Microbiol 2019;85. https://doi.org/10.1128/aem.01516-19.

[19] Gorter de Vries AR, Knibbe E, van Roosmalen R, van den Broek M, de la Torre Cortés P, O'Herne SF, et al. Improving industrially relevant phenotypic traits by engineering chromosome copy number in *Saccharomyces pastorianus*. Front Genet 2020;11. https://doi.org/10.3389/fgene.2020.00518.

[20] Gorter de Vries AR, Couwenberg LGF, van den Broek M, de la Torre Cortés P, ter Horst J, Pronk JT, et al. Allele-specific genome editing using CRISPR–Cas9 is associated with loss of heterozygosity in diploid yeast. Nucleic Acids Res 2018;47:1362–72. https://doi.org/10.1093/nar/gky1216.

[21] Charpentier E, Doudna JA. Rewriting a genome. Nature 2013;495:50–1. https://doi.org/10.1038/495050a.

[22] Jinek M, Chylinski K, Fonfara I, Hauer M, Doudna JA, Charpentier E. A programmable dual-RNA–guided DNA endonuclease in adaptive bacterial immunity. Science 2012;337:816–21. https://doi.org/10.1126/science.1225829.

[23] Al-Attar S, Westra ER, Oost Jvd, Brouns SJJ. Clustered regularly interspaced short palindromic repeats (CRISPRs): the hallmark of an ingenious antiviral defense mechanism in prokaryotes. Biol Chem 2011;392:277–89. https://doi.org/10.1515/bc.2011.042.

[24] Brouns SJJ, Jore MM, Lundgren M, Westra ER, Slijkhuis RJH, Snijders APL, et al. Small CRISPR RNAs guide antiviral defense in prokaryotes. Science 2008;321:960–4. https://doi.org/10.1126/science.1159689.

[25] DiCarlo JE, Norville JE, Mali P, Rios X, Aach J, Church GM. Genome engineering in *Saccharomyces cerevisiae* using CRISPR-Cas systems. Nucleic Acids Res 2013;41:4336–43. https://doi.org/10.1093/nar/gkt135.

[26] Gorter de Vries AR, de Groot PA, van den Broek M, Daran J-MG. CRISPR-Cas9 mediated gene deletions in lager yeast *Saccharomyces pastorianus*. Microb Cell Factor 2017;16:222. https://doi.org/10.1186/s12934-017-0835-1.

[27] Lee ME, DeLoache WC, Cervantes B, Dueber JE. A highly characterized yeast toolkit for modular, multipart assembly. ACS Synth Biol 2015;4:975–86. https://doi.org/10.1021/sb500366v.

[28] Engler C, Kandzia R, Marillonnet S. A one pot, one step, precision cloning method with high throughput capability. PLOS ONE 2008;3:e3647. https://doi.org/10.1371/journal.pone.0003647.

[29] Gibson DG, Young L, Chuang R-Y, Venter JC, Hutchison CA, Smith HO. Enzymatic assembly of DNA molecules up to several hundred kilobases. Nat Methods 2009;6:343–5. https://doi.org/10.1038/nmeth.1318.

[30] Juergens H, Varela JA, Gorter de Vries AR, Perli T, Gast VJM, Gyurchev NY, et al. Genome editing in *Kluyveromyces* and *Ogataea* yeasts using a broad-host-range Cas9/gRNA co-expression plasmid. FEMS Yeast Res 2018:18. https://doi.org/10.1093/femsyr/foy012.

[31] Botman D, de Groot DH, Schmidt P, Goedhart J, Teusink B. *In vivo* characterisation of fluorescent proteins in budding yeast. Sci Rep 2019;9:2234. https://doi.org/10.1038/s41598-019-38913-z.

[32] Gietz DR, Woods RA. Transformation of yeast by lithium acetate/single-stranded carrier DNA/polyethylene glycol method. Methods Enzymol 2002;350:87–96. https://doi.org/10.1016/S0076-6879(02)50957-5.

[33] Lõoke M, Kristjuhan K, Kristjuhan A. Extraction of genomic DNA from yeasts for PCR-based applications. BioTechniques 2011;50:325–8. https://doi.org/10.2144/000113672.

[34] Li H. Aligning sequence reads, clone sequences and assembly contigs with BWA-MEM. arXiv: Genom 2013.

[35] Danecek P, Bonfield JK, Liddle J, Marshall J, Ohan V, Pollard MO, et al. Twelve years of SAMtools and BCFtools. Gigascience 2021;10. https://doi.org/10.1093/gigascience/giab008.

[36] Quinlan AR, Hall IM. BEDTools: a flexible suite of utilities for comparing genomic features. Bioinformatics 2010;26:841–2. https://doi.org/10.1093/bioinformatics/btq033.

[37] Marçais G, Delcher AL, Phillippy AM, Coston R, Salzberg SL, Zimin A. MUMmer4: A fast and versatile genome alignment system. PLOS Comput Biol 2018;14:e1005944. https://doi.org/10.1371/journal.pcbi.1005944.

[38] Langdon QK, Peris D, Baker EP, Opulente DA, Nguyen HV, Bond U, et al. Fermentation innovation through complex hybridization of wild and domesticated yeasts. Nat Ecol Evol 2019;3:1576–86. https://doi.org/10.1038/s41559-019-0998-8.

[39] Okuno M, Kajitani R, Ryusui R, Morimoto H, Kodama Y, Itoh T. Next-generation sequencing analysis of lager brewing yeast strains reveals the evolutionary history of interspecies hybridization. DNA Res 2016;23:67–80. https://doi.org/10.1093/dnares/dsv037.

[40] Nijkamp JF, van den Broek MA, Geertman J-MA, Reinders MJT, Daran J-MG, de Ridder D. De novo detection of copy number variation by co-assembly. Bioinformatics 2012;28:3195–202. https://doi.org/10.1093/bioinformatics/bts601.

[41] Bamforth CW, Kanauchi M. Enzymology of vicinal diketone reduction in brewer's yeast. J Inst Brew 2004;110:83–93. https://doi.org/10.1002/j.2050-0416.2004.tb00187.x.

[42] Godtfredsen SE, Ottesen M. Maturation of beer with α-acetolactate decarboxylase. Carlsberg Res Commun 1982;47:93–102. https://doi.org/10.1007/BF02914029.

[43] Blomqvist K, Suihko M-L, Knowles J, Penttilä M. Chromosomal integration and expression of two bacterial α-acetolactate decarboxylase genes in brewer's yeast. Appl Environ Microbiol 1991;57:2796–803. https://doi.org/10.1128/aem.57.10.2796-2803.1991.

[44] Sone H, Fujii T, Kondo K, Shimizu F, Tanaka J, Inoue T. Nucleotide sequence and expression of the *Enterobacter aerogenes* α-acetolactate decarboxylase gene in brewer's yeast. Appl Environ Microbiol 1988;54:38–42. https://doi.org/10.1128/aem.54.1.38-42.1988.

[45] Yamano S, Tomizuka K, Sone H, Imura M, Takeuchi T, Tanaka J, et al. Brewing performance of a brewer's yeast having α-acetolactate decarboxylase from *Acetobacter aceti subsp. xylinum*. J Biotechnol 1995;39:21–6. https://doi.org/10.1016/0168-1656(94)00135-Y.
[46] Fujii T, Kondo K, Shimizu F, Sone H, Tanaka J, Inoue T. Application of a ribosomal DNA integration vector in the construction of a brewer's yeast having α-acetolactate decarboxylase activity. Appl Environ Microbiol 1990;56:997–1003. https://doi.org/10.1128/aem.56.4.997-1003.1990.
[47] Suihko ML, Blomqvist K, Penttilä M, Gisler R, Knowles J. Recombinant brewer's yeast strains suitable for accelerated brewing. J Biotechnol 1990;14:285–300. https://doi.org/10.1016/0168-1656(90)90113-p.
[48] Knijnenburg TA, Daran J-MG, van den Broek MA, Daran-Lapujade PAS, de Winde JH, Pronk JT, et al. Combinatorial effects of environmental parameters on transcriptional regulation in *Saccharomyces cerevisiae*: a quantitative analysis of a compendium of chemostat-based transcriptome data. BMC Genom 2009;10:53. https://doi.org/10.1186/1471-2164-10-53.
[49] Yamano S, Tanaka J, Inoue T. Cloning and expression of the gene encoding α-acetolactate decarboxylase from *Acetobacter aceti ssp. xylinum* in brewer's yeast. J Biotechnol 1994;32:165–71. https://doi.org/10.1016/0168-1656(94)90179-1.
[50] Guo W, He X, Tie C, Zhang B. Expression of α-acetolactate decarboxylase gene from *Bacillus subtilis* in brewer's yeast. Wei sheng wu xue bao = Acta Microbiol Sin 2001;41:105–8.
[51] Godtfredsen SE, Rasmussen AM, Ottesen M, Mathiasen T, Ahrenst-Larsen B. Application of the acetolactate decarboxylase from *Lactobacillus casei* for accelerated maturation of beer. Carlsberg Res Commun 1984;49:69. https://doi.org/10.1007/BF02913966.
[52] Kuijpers NGA, Solis-Escalante D, Bosman L, van den Broek M, Pronk JT, Daran J-M, et al. A versatile, efficient strategy for assembly of multi-fragment expression vectors in *Saccharomyces cerevisiae* using 60 bp synthetic recombination sequences. 47-47 Microb Cell Factor 2013;12. https://doi.org/10.1186/1475-2859-12-47.
[53] Ma H, Marti-Gutierrez N, Park SW, Wu J, Lee Y, Suzuki K, et al. Correction of a pathogenic gene mutation in human embryos. Nature 2017;548:413–9. https://doi.org/10.1038/nature23305.
[54] Lombardi L, Bergin SA, Ryan A, Zuniga-Soto E, Butler G. CRISPR-Cas9 editing induces loss of heterozygosity in the pathogenic yeast *Candida parapsilosis*. mSphere 2022:e0039322. https://doi.org/10.1128/msphere.00393-22.
[55] Wach A, Brachat A, Pöhlmann R, Philippsen P. New heterologous modules for classical or PCR-based gene disruptions in *Saccharomyces cerevisiae*. Yeast 1994;10:1793–808. https://doi.org/10.1002/yea.320101310.
[56] Baudin A, Ozier-Kalogeropoulos O, Denouel A, Lacroute F, Cullin C. A simple and efficient method for direct gene deletion in *Saccharomyces cerevisiae*. Nucleic Acids Res 1993;21:3329–30. https://doi.org/10.1093/nar/21.14.3329.
[57] Bolat I, Romagnoli G, Zhu F, Pronk JT, Daran JM. Functional analysis and transcriptional regulation of two orthologs of *ARO10*, encoding broad-substrate-specificity 2-oxo-acid decarboxylases, in the brewing yeast *Saccharomyces pastorianus* CBS1483. FEMS Yeast Res 2013;13:505–17. https://doi.org/10.1111/1567-1364.12051.
[58] Duong CT, Strack L, Futschik M, Katou Y, Nakao Y, Fujimura T, et al. Identification of *Sc*-type *ILV6* as a target to reduce diacetyl formation in lager brewers' yeast. Metab Eng 2011;13:638–47. https://doi.org/10.1016/j.ymben.2011.07.005.
[59] Hansen EH, Møller BL, Kock GR, Bünner CM, Kristensen C, Jensen OR, et al. De novo biosynthesis of vanillin in fission yeast (*Schizosaccharomyces pombe*) and baker's yeast (*Saccharomyces cerevisiae*). Appl Environ Microbiol 2009;75:2765–74. https://doi.org/10.1128/aem.02681-08.
[60] Denby CM, Li RA, Vu VT, Costello Z, Lin W, Chan LJG, et al. Industrial brewing yeast engineered for the production of primary flavor determinants in hopped beer. Nat Commun 2018;9:965. https://doi.org/10.1038/s41467-018-03293-x.
[61] Arroyo-López FN, Orlić S, Querol A, Barrio E. Effects of temperature, pH and sugar concentration on the growth parameters of *Saccharomyces cerevisiae*, *S. kudriavzevii* and their interspecific hybrid. Int J Food Microbiol 2009;131:120–7. https://doi.org/10.1016/j.ijfoodmicro.2009.01.035.
[62] Gangl H, Batusic M, Tscheik G, Tiefenbrunner W, Hack C, Lopandic K. Exceptional fermentation characteristics of natural hybrids from *Saccharomyces cerevisiae* and *S. kudriavzevii*. Nat Biotechnol 2009;25:244–51. https://doi.org/10.1016/j.nbt.2008.10.001.
[63] Borneman AR, Desany BA, Riches D, Affourtit JP, Forgan AH, Pretorius IS, et al. The genome sequence of the wine yeast *VIN7* reveals an allotriploid hybrid genome with *Saccharomyces cerevisiae* and *Saccharomyces kudriavzevii* origins. FEMS Yeast Res 2012;12:88–96. https://doi.org/10.1111/j.1567-1364.2011.00773.x.
[64] Hawthorne D, Philippsen P. Genetic and molecular analysis of hybrids in the genus *Saccharomyces* involving *S. cerevisiae, S. uvarum* and a new species, *S. douglasii*. Yeast 1994;10:1285–96. https://doi.org/10.1002/yea.320101005.
[65] Le Jeune C, Lollier M, Demuyter C, Erny C, Legras J-L, Aigle M, et al. Characterization of natural hybrids of *Saccharomyces cerevisiae* and *Saccharomyces bayanus var. uvarum*. FEMS Yeast Res 2007;7:540–9. https://doi.org/10.1111/j.1567-1364.2007.00207.x.
[66] Masneuf I, Hansen J, Groth C, Piskur J, Dubourdieu D. New hybrids between *Saccharomyces sensu stricto* yeast species found among wine and cider production strains. Appl Environ Microbiol 1998;64:3887–92. https://doi.org/10.1128/aem.64.10.3887-3892.1998.
[67] Ortiz-Merino RA, Kuanyshev N, Braun-Galleani S, Byrne KP, Porro D, Branduardi P, et al. Evolutionary restoration of fertility in an interspecies hybrid yeast, by whole-genome duplication after a failed mating-type switch. PLOS Biol 2017;15:e2002128. https://doi.org/10.1371/journal.pbio.2002128.
[68] Louis VL, Despons L, Friedrich A, Martin T, Durrens P, Casarégola S, et al. *Pichia sorbitophila*, an interspecies yeast hybrid, reveals early steps of genome resolution after polyploidization. G3 (Bethesda) 2012;2:299–311. https://doi.org/10.1534/g3.111.000745.
[69] Entian K-D, Kötter P. 25 yeast genetic strain and plasmid collections. In: Stansfield I, Stark MJR, editors. Methods in Microbiology, vol. 36. Academic Press; 2007. p. 629–66.
[70] Dunn B, Sherlock G. Reconstruction of the genome origins and evolution of the hybrid lager yeast *Saccharomyces pastorianus*. Genome Res 2008;18:1610–23. https://doi.org/10.1101/gr.076075.108.
[71] Hassing E-J, de Groot PA, Marquenie VR, Pronk JT, Daran J-MG. Connecting central carbon and aromatic amino acid metabolisms to improve de novo 2-phenylethanol production in *Saccharomyces cerevisiae*. Metab Eng 2019;56:165–80. https://doi.org/10.1016/j.ymben.2019.09.011.